KADIR HAS UNIVERSITY

GRADUATE SCHOOL OF SCIENCE AND ENGINEERING

IN SILICO DESIGN OF NOVEL AND HIGHLY SELECTIVE
CYCLOOXYGENASE-2 INHIBITORS

TUĞBA MEHMETOĞLU

January, 2014

Tuğba Mehmetoğlu

M.Sc. Thesis

2014

IN SILICO DESIGN OF NOVEL AND HIGHLY SELECTIVE

CYCLOOXYGENASE-2 INHIBITORS

TUĞBA MEHMETOĞLU

Submitted to the Graduate School of Science and Engineering

in partial fulfillment of the requirements for the degree of

Master of Science

in

Computational Biology and Bioinformatics

KADIR HAS UNIVERSITY

January, 2014

KADIR HAS UNIVERSITY GRADUATE SCHOOL OF SCIENCE AND
ENGINEERING

[*IN SILICO* DESIGN OF NOVEL AND HIGHLY SELECTIVE
CYCLOOXYGENASE-2 INHIBITORS]

[TUĞBA MEHMETOĞLU]

APPROVED BY:

[Prof. Dr. Kemal Yelekçi (Advisor)   KHAS

[Prof. Dr. Safiye Sağ Erdem   MÜ   ]

[Asst. Prof. Dr. Hatice Bahar Şahin   KHAS _____]

APPROVAL DATE: 10/Jan/2014

i

"I, Tuğba Mehmetoğlu, confirm that the work presented in this thesis is my own. Where information has been derived from other sources, I confirm that this has been indicated in the thesis."

Abstract

IN SILICO DESIGN OF NOVEL AND HIGHLY SELECTIVE

CYCLOOXYGENASE-2 INHIBITORS

TUĞBA MEHMETOĞLU

Master of Science in Computational Biology and Bioinformatics

Advisor: Prof. Dr. Kemal Yelekçi

January, 2014

For many years, prevention of inflammation is achieved by inhibition of both cyclooxygenase (COX) enzymes; the eventual outcome is gastrointestinal toxicity. Selective inhibitor design for COX-2 initialized just after discovery of two distinct types of COX enzymes. Both isoforms of COX show great similarities at the active sites. It is still essential to find more potent, more selective and reversible COX-2 inhibitors.

Crystallographic structures of COX-1 (pdb code: 1Q4G; Ovis aries COX-1 crystallized with Alpha-Methyl-4-Biphenylacetic, resolution 2.00 Å) and COX-2 (pdb code: 3NT1; Mus musculus COX-2 crystallized with naproxen, resolution 1.73 Å) isozymes have paved the way for computational modeling.

In the present work, from receptor cavities of enzyme, suitable scaffolds for both isozyme are generated by using ZINCv12 fragment library. Accelrys 3.1's Discovery Studio Protocols and *de novo* design module were assigned in the derivation process of the scaffolds via link library to produce 1129 analogs. GOLD and AutoDock 4 are used to scan and define poses in catalytic sites of both COX isozymes. Known inhibitors were taken as a reference for verification of modeling studies. The best resultant inhibitors are subjected to ADMET test and validity is confirmed.

Key words: COX-2 inhibitor, structure based drug design, docking, modeling

Özet

BİLGİSAYAR DESTEKLİ İLAÇ TASARIMI KULLANARAK SEÇİCİ
SİKLOOKSİJENAZ-2 İNHİBİTÖRÜ TASARIMI

TUĞBA MEHMETOĞLU

Hesaplamalı Biyoloji ve Biyoinformatik, Yüksek Lisans

Danışman: Prof. Dr. Kemal Yelekçi

Ocak, 2014

Yıllarca, vücutta oluşan enflamasyonu engellemek için her iki COX enzim inhibisyonunun sağlanması gerektiği düşünülmüş ve sonuçta gastrointestinal zehirlenmeler ortaya çıkmıştır. Seçimli COX-2 inhibitör tasarımı, iki ayrı COX enzimi bulunmasından hemen sonra başlamıştır. Her iki enzim de aktif bölgelerinde yüksek benzerlik gösterir. Daha etkili, seçimli ve tersinir COX-2 inhibitör tasarımı çok önemlidir.

COX-1 (pdb kodu: 1Q4G; Alfa-Metil-4-Bifenilasetik asit ile koyun COX-1 enzimi, çözünürlük 2.00 Å) ve COX-2 (pdb kodu: 3NT1; naproksen ile fare COX-2 enzimi, çözünürlük 1.73 Å) kristalleri *in silico* olarak hesaplamalı modellemenin yolunu açmıştır.

Bu çalışmada reseptör oyuklarından her iki enzim içinde ZINCv12 parçacık kütüphanesi yardımı ile uygun iskelet yapılar oluşturulmuş, küçük grupları Accelrys 3.1 Discovery Studio protokolleri ve *de novo* dizayn modülü ile farklı pozisyonlarda kullanılarak 1129 analog elde edilmiştir. GOLD ve Autodock 4 kullanılarak tarama gerçekleştirilmiş ve bağlanma pozları belirlenmiştir. Piyasada bulunan bilinen inhibitörler çalışmada temel referans olarak alınmıştır. En iyi çıkan inhibitörler ADMET testine tabi tutulmuş ve geçerli sayılmıştır.

Anahtar Kelimeler: Siklooksijenaz-2 inhibitörü, yapı odaklı ilaç tasarımı, docking, modelleme

Acknowledgements

Table of Contents

List of Figures

List of Tables

1. Chapter 1: Properties of Cyclooxygenases

1.1 Introduction

In the 1990's a noteworthy breakthrough was emerged from sophisticated molecular and cellular biological studies that; two cyclooxygenase (COX) enzyme systems present and taking part in steps of the generating of prostanoids; COX-1 products regulates biological functions on the other hand COX-2 products regulate generation of prostaglandins taking part in inflammation, aching and fever. Specifically inhibiting COX-2 products have been the principal aim for remedying rheumatoid and osteo-arthritis and other arthritic diseases, dental and surgical pain in post-operative states, dysmenorrhoea, and acute injuries. According to World Health Organization (WHO) population statistics; 10-50% of individuals suffer from musculoskeletal disorders and the majority suffer from pain. Approximately all will require Non-Steroidal Anti-Inflammatory Drugs (NSAIDs) and other analgesics for their pain management[1].

The focus of this thesis is defining the necessary inhibitors for the management of COX associated infections. Due to high homology between the active sites of two isoenzymes, selectivity of the resultant drug is the most important target. Searching for new, reversible and highly selective COX-2 inhibitors via *in silico* drug design methods is the main objective of this study.

Synthesizing new drugs, even with rational drug design methods, takes ages to find effective solutions. In addition, needed effort and project budget could be unpredictable. These kinds of studies may end up without successful result. Computational modeling studies are more economic and faster alternative to start with best possible pathway. This generates an opportunity to start searching

1

candidate drug via computational technique rather than following the traditional method to find better solutions[2].

1.1 Mechanism of COX enzymes

Both a broad array of stimuli in the cell and mobilization of calcium activate phospholipase A_2. It is widely known that vast majority of biologically active lipids are originated from esterified arachidonic acid (AA) by the engagement of oxidative enzymes. AA biotransformation (Figure-1.1) is catalyzed by phospholipase A_2, to eventually produce unoccupied arachidonate, which is the preliminary rate-limiting step throughout formation of sequential eicosanoids including prostanoids (prostaglandins E_2, D_2, $F_{2\alpha}$, I_2, and thromboxane A_2). Crucial enzyme group; prostaglandin endoperoxide synthases (also known as COX) and hydroperoxidase (HOX) catalyze the first assigned stage in the transformation of AA into the prostanoid associated metabolites[3]. COX enzymes maintain two distinctive catalytic actions: (1) a cyclooxygenase that biotransforms AA and two molecules of molecular oxygen to generate PGG_2 and (2) a peroxidase (HOX) that reduces PGG_2 to PGH_2. Both actions necessitate heme groups that exist one per enzyme subunit[4].
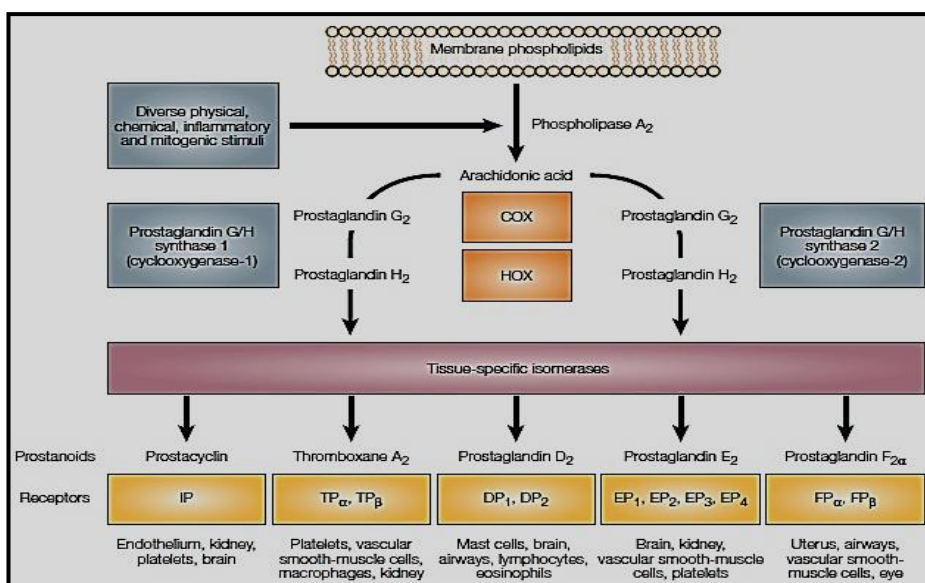
Figure 1. 1: Schematic view of Prostanoids Mechanism adapted from FitzGerald[5].

1.2 COX isoenzymes

At the moment, there are three types of COX enzymes known; namely, COX-1, COX-2 and COX-3. Starting with COX-1; it yields products, which largely provide 'housekeeping' functions, such as gastric cyto-protection as well as homeostasis. By contrast, expression of COX-2 is strictly controlled by cytokines and mitogens, and considered to be essential for stimulating the inflammatory response in prostaglandin formation, mostly taking place in inflammation and cancer. Nevertheless, prostaglandins, which are originated through COX-1, can contribute to inflammation[6]. COX-1 is expressed in several tissues such as brain, liver, lung, spleen, kidney, stomach as well as other gastrointestinal tract tissue; but not in renal medulla. Basically, mRNA for COX-2 was not noticeable in tissues except brain[7,8]. However, immunocytochemical localization of COX-1 and COX-2 indicated that both isoforms were present in the rat stomach, in the alveolar, peritoneal macrophages of mice and in amniotic epithelium[8-10]. Also constitutive expression of COX-2 in the brain and kidneys is well documented and expression of COX-2 increased in labor[7,11].At cellular level, both COX-1 and COX-2 are positioned on the luminal side of the ER, but COX-2 also seems to exist in the nuclear envelope[12]. Despite these variations from the simple hypothesis of bearing two distinct roles, the hypothesis has been the touchstone for rationale drug discovery and development of selective COX-2 inhibitors, which mainly focus on the lateral extension of the hydrophobic channel in the isozyme[3,13].COX-3 is variant of COX-1 and is only detected in dog brain[14].
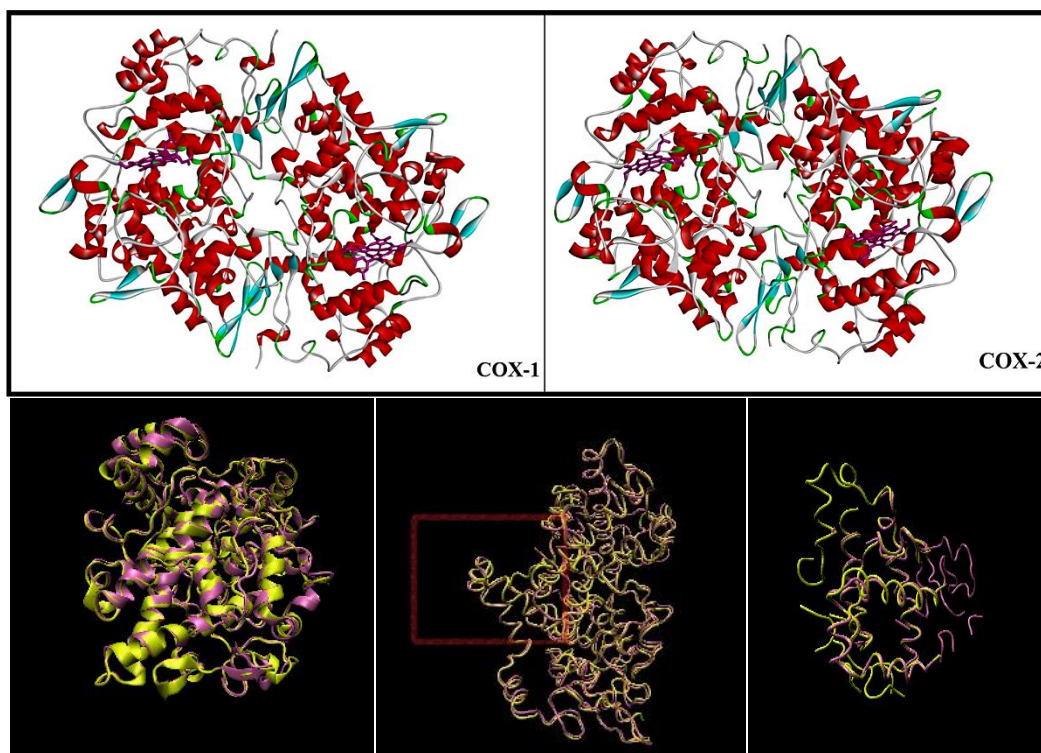
Figure 1. 2: 3-D view of COX-1 and COX-2 retrieved from Accelery's Discovery Studio 3.1and superimpose of them two COX enzymes retrieved from Visual Molecular Dynamics (VMD). COX-1: mauve, COX-2: yellow.

1.3 Structure and Physiochemical Properties of COX enzymes

COX-1and COX-2 (EC 1.14.99.1) are both found in integral membrane protein family. Unlike many membrane related receptors, COX enzymes do not contain hydrophobic membrane penetrating arrangements by means of primary structure; instead they seem to have monotopic interaction through three N-terminal mini α-helices, which are amphipathic (Figure-1.2).[15] Active site of the cyclooxygenase is confined in 25 Å constricted hydrophobic channel that elongates throughout the membrane binding motif up via the epicenter of the protein terminating at the heme binding site, which locates in cytoplasm, adjoining to the peroxidase active site. At upper end of channel is majorly consisted of Tyr 385 and Ser 530. Residue Arg 120 is located in the middle of the channel, in appropriate position to make interaction

with either the arachidonate carboxylate or, as was comprehended in the ovine X-ray structure which is with flubiprofen, the carboxylate of an NSAID (Figure-1.3)[16].
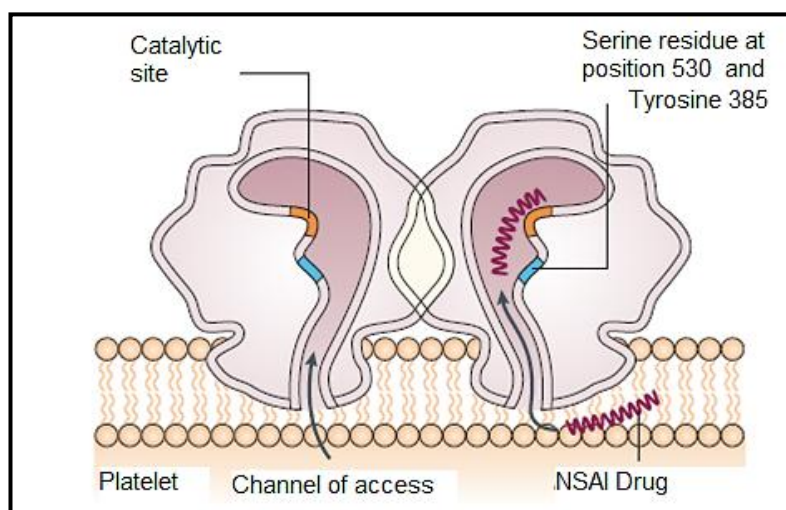
Figure 1. 3: Binding site of COX enzymes.

COX-1 enzyme isolated from sheep, mouse and human demonstrates roughly 90% homology at amino acid level. COX-1 and COX-2 have approximately 60% homology by means of amino acid sequence in the same species of sheep, mouse and human[17]. Excluding N- and C-termini of the COX enzymes, since two proteins are mostly dissimilar in these regions, they are approximately 75% identical. Human COX-1 has 576 amino acid and the predicted molecular weight of subunit is 65kDa, whereas ovine COX-1 has 580 amino acid[18,19]. Molecular weight increases up to 72kDa by the action of post-translational modification occurring at glycosylation sites found within three high mannose oligosaccharides[19]. In COX-2, mouse homolog has 587 amino acid and a supplementary glycosylation site exists on the C-terminal with 18-amino acid insert in human [16,20]. Fractional glycosylation arises at C-terminal and COX-2 seems as a 72kDa/74kDadouble band on SDS-gel. Both enzymes preserve activity after removal of the sugars, but they become less stable[20]. The N-terminus includes signal sequences of 25 (COX-1) and 17 (COX-2) amino

acids that lacks in the processed polypeptide. A remarkable variation among isoforms exists close to the C-terminus of COX-2 as an 18-amino acid insertion. This exceptional sequence has been used to develop COX-2 targeted antibodies in the market and also for rational drug design (Figure 1.4)[21].
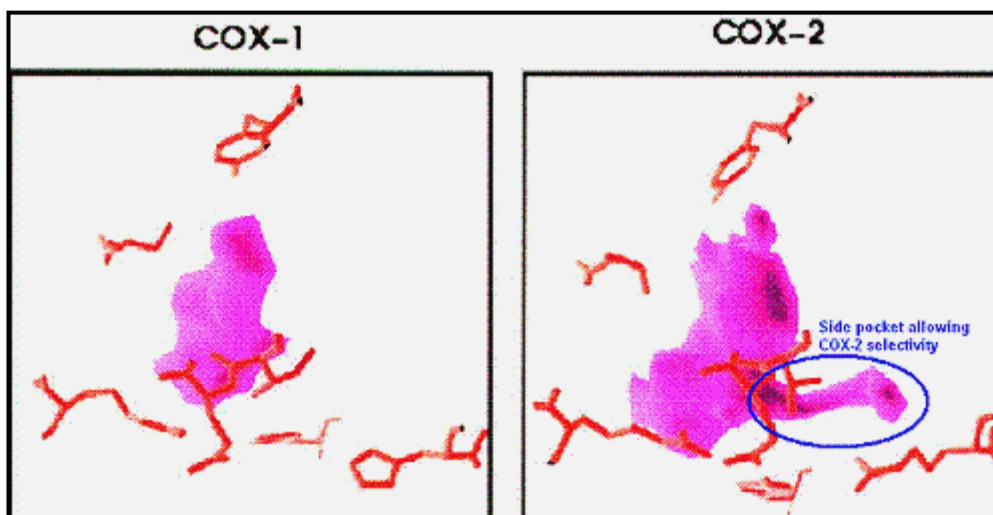
Figure 1. 4: Schematic view of selectivity feature of COX-2 against COX-1

1.4 COX enzymology

COX-1 was the first isoenzyme isolated from sheep seminal vesicles as a sedentary homodimer. Adding heme group, one per each dimer subunit, is involved for catalytic activities. At the end of peroxidase reaction of resting heme, a ferryl-oxo complex (Fe^{+4}-O) is produced in COX enzyme (the iron is ferric in the inactive enzyme and is thermodynamically unable to oxidize Tyr385). Inactive Fe is represented as a radical cation Fe^{+4} intermediate that may either take a hydrogen atom away from Tyr385 or go through a two-electron reducing back to the sedentary state of Fe^{+3}enzyme (Figure 1.5). Tyrosine radical is supposed to be initiator of the COX reaction. A study with T385F mutant in COX states that; mutant enzyme loses

its cyclooxygenase activity nevertheless retains its peroxidase activity that is compatible with the suggested mechanism [22,23].
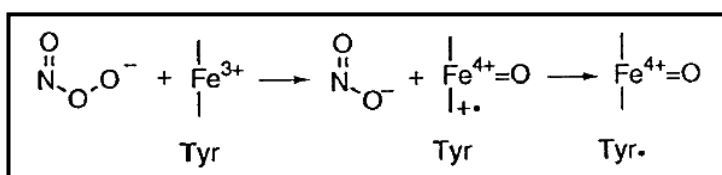
Figure 1. 5: Equation showing reduce state of Fe adapted from Marnett et al[24].

The heme irons of most HOXs are organized by the four nitrogens of the protoporphyrin ring and at the fifth coordination position by the Nδ atoms of the imidazole group of the proximal histidine. In some cases, the iron is also coordinated at the sixth position with either a small inorganic ion or water. Distal histidine located near the sixth coordination position pulls a proton from the peroxide substrate and this becomes substrate for COX. His 207, Gln 203 and His 388 are important for catalysis and heme coordination (Figure-6)[25-27].
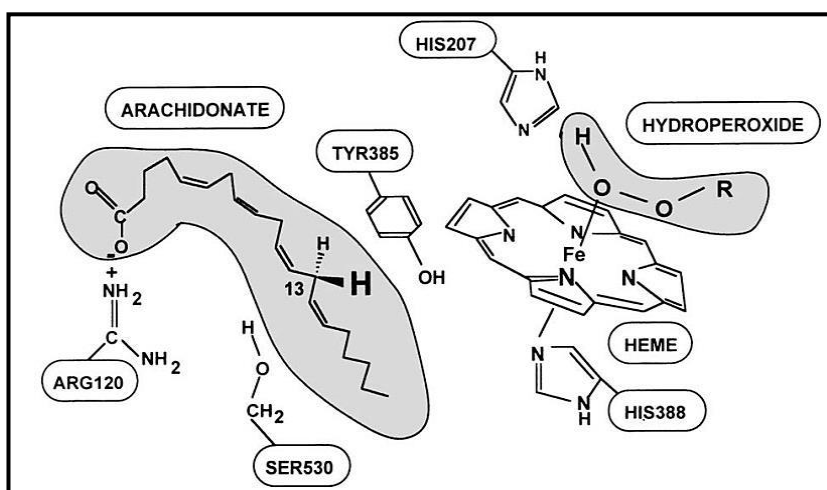
Figure 1. 6: Interacting residue of COX and HOX adapted from Smith et al[28].

1.5 Crystallographic and structural properties of COX enzymes

Many crystallization, computational simulation and molecular modeling studies deduce very important data that contribute to design of COX inhibitors. Both COX isoenzymes of ovine and mouse crystallizes as dimer, whereas human COX enzymes crystallizes as four chains[16,18,29]. COX enzyme has two sites; one is for reducing Fe^{+4} to Fe^{+3} by peroxide (HOX), and the other is catalytic site for AA. These 2 sites elongate in opposite direction (Figure-1.7)[3].Active site of COX-2 is nearly 20% larger and more accommodating than that of COX-1 .This difference in active site size and shape is due to three amino acid differences between COX-1 and COX-2: Ile523 to Val523 in the first shell of the active site, Ile 434 to Val434 and His513 to Arg513 in the covering second shell. Both COX entrance cavity volume is about 25Å for each monomer of hydrophobic channel that originates at the membrane-binding domain (MBD) that is assembled from residues 111-122 and projects into the core of the globular domain[13].

COX-2 has 2090 $Å^3$ cavity volume. A number of amino acids constituting the superior half of the channel have a key role in cyclooxygenase catalysis. Active site of COX-2 is restricted by H-bonding network done by side chains of Arg 120, Glu524, Tyr355 and Arg513. Twenty-four residues reside within the hydrophobic cyclooxygenase active site with only one difference between COX isozymes—Ile at position 523 in COX-1 and Val at position 523 in COX-2.Amino acids exist in the hydrophobic cyclooxygenase active site channel include; Leu117, Arg120, Phe205, Phe209, Val344, Ile345, Tyr348, Val349, Leu352,Ser353, Tyr355, Leu359, Phe381, Leu384, Tyr385, Trp387, Phe518, Ile/Val523,Gly526, Ala527, Ser530, Leu531, Gly533, Leu534.Only three of the channel residues are polar (Arg120, Ser353, and Ser530). Arg120 has an important gate like property for binding drug to COX-2.

Selectivity of COX-2 comes probably from hydrogen bonding between; His90 Arg513 and Tyr355. H-bond between Arg513-Glu524 was relaxed during drug entrance to COX-2 cavity. Volume of designed drug should not exceeds the cavity volume or at most 70% should be covered in order to be effective agent[30].
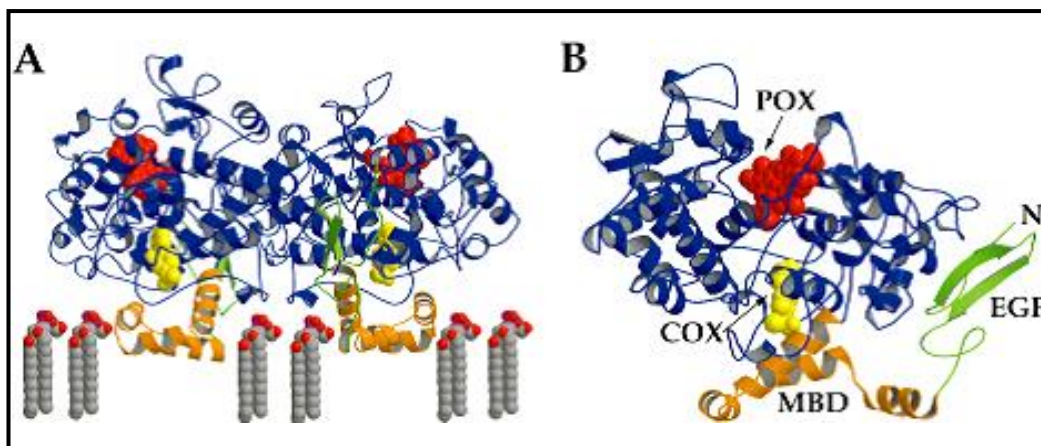
Figure 1. 7:A)General view of COX-enzyme, B)Binding site of COX enzymes pointed with arrow as COX adapted from Ref[3]. POX: peroxide binding site, EGF: Epidermal Growth Factor, MBD: Membrane binding domain.

2. Chapter 2: COX inhibition

Inhibiting prostanoid groups in the metabolism provokes toxicity and this is well documented with the fact that widespread and non-specific inhibition of COX enzymes in the body creates toxicity (Figure-8). In several studies, gastrointestinal tract and renal damage is noticeably demonstrable both in animal models and clinical trials with COX inhibitors namely NSAID[7,31,32].A proposed mechanism of inhibition of COX activity is changing the route to other arachidonic acid using pathways such as lipoxygenase production (e.g., 5-lipoxygenase, 12-lipoxygenase, and 15-lipoxygenase). Treatment of COX-2 enzyme with aspirin seems to inhibit the production of prostanoid, essentially seems to induce the production of 15-HETE[33].
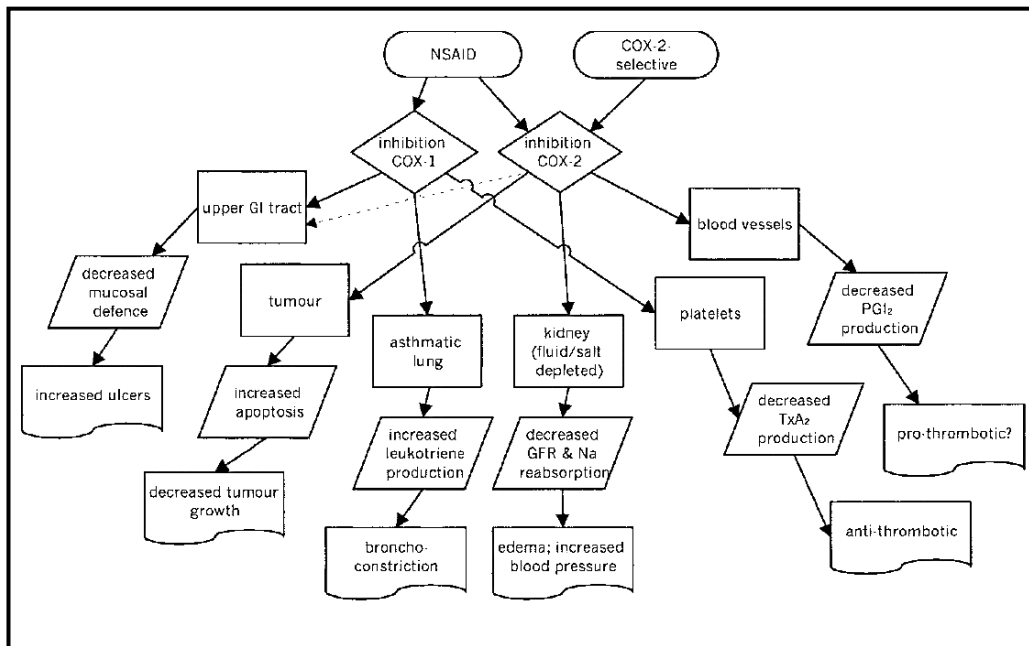
Figure 1. 8: Outcomes of COX-1 and/or COX-2 inhibition adapted from Ref[34].

2.1 Mechanisms of COX Inhibition

There are numerous proposed mechanisms for competitive inhibition of prostaglandins by inhibiting the cyclooxygenase reaction, which are;

1. Limiting the concentration of substrate that are either arachidonate or O_2radical[35],

2. Inhibiting oxidative activation by declining the concentration of hydroperoxide initiator below 10 nM[36],

3. Reducing catalytically dynamic enzyme back to the inert ground state[37,38],

4. Prevention of substrate (arachidonate) binding.

The fourth category, inhibition of substrate binding, seems to be the general target of intervention for the common of NSAIDs. Nevertheless, the other forms of intervention may have a noteworthy influence on *in vivo* efficacy of an inhibitor, besides suggesting an alternative method for inhibition of prostanoid production. Antagonism for binding at the arachidonate binding site is the major method of inhibition for most of the acidic traditional NSAIDs and inhibition of cyclooxygenase active site does not affect status of HOX activity. The simulation of the arachidonate carboxylate by the acidic function of NSAID suggested in Shen's model is compatible with the X-ray co-crystal structure defined for S-flurbiprofen with ovine COX-1[7]. This structure demonstrates the flurbiprofen carboxylate interacting with Arg120 in mostly lipophilic arachidonate binding channel. Two kinds of inhibition kinetics have been identified for the acidic NSAIDs; reversible and tightly irreversible inhibitors, which includes conformational change and covalent bonding[22].

2.2 Classification of COX inhibitors

COX inhibitors are called as NSAID (Non-steroid Anti-Inflammatory Drug) and there are two class of NSAIDs; traditional and new generation. Traditional NSAID (tNSAID) includes carboxylic acid, carboxamide/oxicam and sulfonanilide group containing inhibitors (Figure-1.9);binding to both COXes, they are non-specific inhibitors. They contain 1 or 2 but not 3 phenyl ring in their structure. Bulky alkyloxy (ethyl vs. methyl) or aryloxy substituents seem to be unfavorable for COX-1 inhibition and these 3 side groups does not exist in tNSAID structure, but in COX-2 specific inhibitors. Compounds possessing a free carboxylate exhibit nonselective COX inhibition and this group exist in tNSAID such as; aspirin, indomethacin, naproxen[24,39,40].

Carboxylic acids

- Salicylates
  Aspirin
  Diflunisal
- Fenamates
  Flufenamic acid
  Mefenamic acid
  Meclofenamic acid
  Tolfenamic acid
- Indole/indene
  acetates
  Indomethacin
  Sulindac
- Phenylacetates
  Diclofenac
  Etodolac
  Ketorolac
  * Lumaricoxib
- Propionates
  Dexibuprofen
  Dexketoprofen
  Flurbiprofen
  Ketoprofen
  Ibuprofen
  Naproxen
  Tiaprofenic acid

Carboxamides or Oxicams

- Oxicams
  Piroxicam
- Carboxamides
  Meloxicam

Sulphonanilides

Nimesulide

Diaryl-substituted pyrazoles/furanones

- Coxibs
  Celecoxib
  Etoricoxib
  Parecoxib
  ** Rofecoxib
  ** Valdecoxib

* Described as a Coxib but is not chemically in this class
** Now withdrawn

Figure 1. 9: Classification of COX-2 specific drugs adapted from Ref[41.]

Selective COX-2 inhibitors such as Celecoxib, Rofecoxib and Valdecoxib have been put into the market as new generation NSAIDs, which are coxib class (Figure-1.10). Coxib stands for **Cox**-**i**nhi**b**itors and these compounds all bear the diaryl heterocyclic structural features. The pharmacophore of diarylheterocycles inhibitors is distinguished by a central carboxylic or heterocyclic ring system carrying two vicinal aryl moieties and one benzene ring substituted with methylsulfonyl or aminosulfonyl group at the para position. The major difference in the new generation compounds is the structure of the central ring and arylsulphonyl group for selectivity purpose. Thus, modification in the central ring will direct us to novel COX-2 inhibitors. Indole ring comprises a significant prototype for drug design from tNSAIDs such as indomethacin and indoxole[42,43].
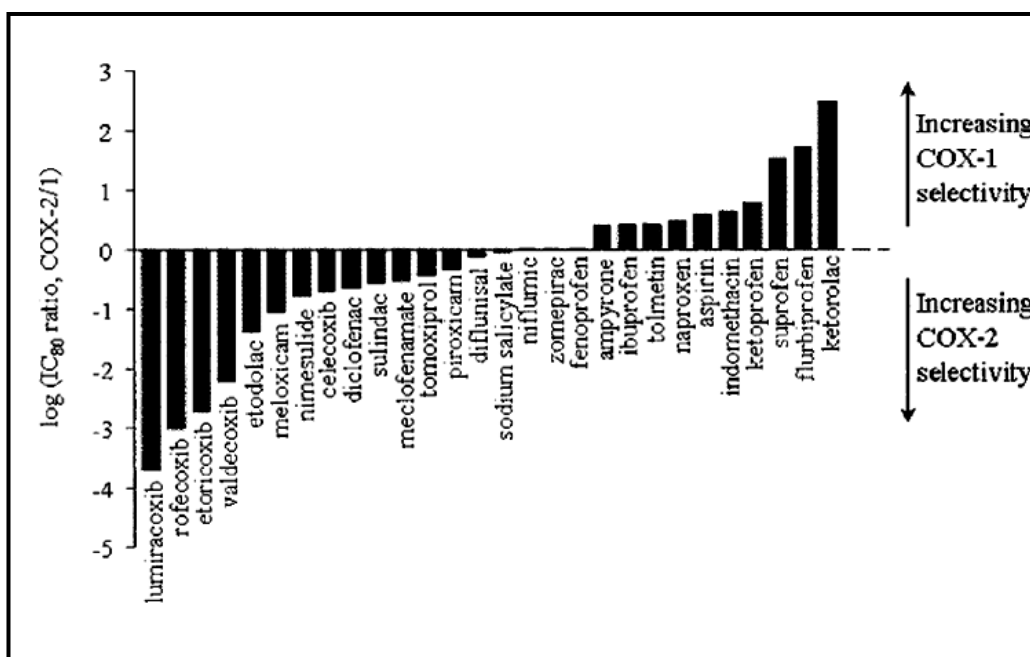
Figure 1. 10: Graph representing COX2/COX1 selectivity via IC_{80} values adapted from Ref[34].

3. Chapter 3: Methods and Procedures Used in Molecular Modeling

3.1 Introduction

Inhibition of an enzyme is the method that drug follows to decrease enzyme's activity. Drugs should achieve to inhibit the target enzyme within a low concentration range and should not crosstalk with any other enzymes that are functioning in metabolism and also not crosstalk with compounds that are known as strong inhibitors. These properties are critical to obtain drugs that are non-toxic to both metabolism and individual or at least have less or non-side effect.

In this study, Structure Based Drug Design (SBDD) is the major method used. Initially, structural information of a molecule in terms of coordinates can be assembled from NMR or X-Ray crystallography. RCSB Protein Data Bank currently comprises at least 90000 crystal structures with their 3D data. All these information is accessible for molecular modeling applications and also for computational biology studies. In order to achieve SBDD goal, Accelrys Discovery Studio Client 3.1[44,45] was used. This method includes two main follow up protocols: *De novo Receptor* and *De novo evolution*.

The former protocol depends on searching for complementary small molecules that best bind to interaction sites, which are determined by receptor cavity (active sites atom). This protocol does not contain scaffold however it selects scaffold from a library according to some rules. LUDI is a procedure for the *de novo* design of

ligands for proteins in Accelrys Discovery Studio Client 3.1. It is a practical method for screening vast number of candidates. This procedure evaluates a geometrical fit of candidate compounds into the binding cavity and computes other determinants of good binding such bas hydrogen bonds, lipophilic interactions, ionic interactions, and acylic interactions. LUDI scoring functions statistically assesses the fit of all likely ligands. $\Delta G = \Delta G_o + \Delta G_{hbf}(\Delta R)f(\Delta\alpha) + \Delta G_{ionf}(\Delta R)f(\Delta\alpha) + \Delta G_{lipo}A_{lipo} + \Delta G_{rot}NR$ ΔG; ΔG_o stands for the contribution to the binding energy that does not straight relate to any defined interactions with the receptor (i. e. the involvement of binding energy due to loss of transitional and rotational entropy of the fragment), ΔG_{hb} and ΔG_{ion} stands for the contribution from an ideal hydrogen bond and unperturbed ionic interactions, respectively, ΔG_{lipo} stands for the contribution from lipophilic interactions which is proportional to the lipophilic surface A_{lipo} , ΔG_{rot} stands for the contribution due to freezing of internal degrees of freedom in the fragment, NR is the number of acylic bonds, ΔR is the divergence of the hydrogen bond length from the ideal value that is 1.9 Å, Δa is the divergence of the hydrogen bond angle from ideal value 180°. Generally a higher LUDI score (0-1000 in range) corresponds to a higher affinity and stronger binding of a ligand to the receptor. During the search and fit computation LUDI scores are calculated and also the energy estimations, or scores, for each conformation searched for the fragments in the library are determined. The DS LUDI was used extensively in this work, which quests fragment libraries and yields molecules that fit the requirements of the defined interaction sites. Ligand-receptor complexes may be evaluated using the empirical scoring functions available from the LUDI algorithm. The score is a sum of five contributions: ideal hydrogen bonds, perturbed ionic interactions (interaction of donor/acceptor in the receptor, e.g., COO^-, or NH_3^+), lipophilic interactions, the freezing of internal degrees of

freedom of the ligand, and the loss of translational and rotational entropy of the ligand. In receptor mode, during the "search and fit" the LUDI program also determines the energy estimates, or scores, for each conformation of the selected fragments in the library. The fragments are ranked by energy estimate, and the best are returned in the hit list. This hit list can then be inspected for the selection of candidate scaffolds and eventually program yields "*.sd" file for further inspection. In this study, LUDI receptor mode was used against COX-2 and COX-1 enzymes which screened potential lead compounds from more than a million lead compounds in the ZINCv12[46] lead library for their structural and physicochemical properties.

The latter protocol, *de novo evolution* depends on a specified scaffold positioned in a protein site; LUDI is used to identify fragments that may be covalently fused to the scaffold and yields a collection of molecules with high LUDI scores. Fragment selection and construction for new molecules relies on the mode. Finally, all new compounds will be further refined using CHARMm and scored by MM-PBSA/GBSA[47]. Using ZINC and Accelrys 3.1 fragment-based libraries, which contain about 400,000 fragments, eventually 1129 potential candidates, were generated.

In this study, *de novo* designed ligands are docked into both COX enzymes *in silico*. None of those compounds has been synthesized or investigated beforehand; which is confirmed by ZINCv12 website.

Docking of ligand and enzyme is the leading virtual screening method to check compound candidates. Objective of the study is discovering the best matching for ligand and receptor by conducting virtual screening. Also docking foresees the binding energy for each ligand and possible binding pose for each ligand embedded in 3D structure of enzyme by using various scoring functions. Fundamental job of scoring function is guessing the interaction or binding affinity and calculating score of affinity between two molecules that are generally an enzyme and candidate compound[48]. Primarily the method is formed as which tracked by locating the enzyme and the candidate compound within that system. By performing minimization step, the lowest free energy of binding is simulated as induced fit[49]. Two major standards exist to be accomplished. The first one is shape consistency occurring between candidate compound and enzyme, the second one is interrelation between them. Devoid of the fitting interrelation leads one to have useless fitting geometric structures.

Currently available docking programs include three major parts: system depiction, searching of conformational volume, and the classification of the potential resolutions. The best suitable results were retrieved based on two criteria; the first one is having an efficient search algorithm that gives the less faulty results and the second one is having improved scoring function. Nowadays, there is a good number of conformational search algorithms available, however getting scores from the prospective result is the main problematic fact to detect the best software combination[50,51]. Yet designed for particular experimentations, using just one docking tool only for conformational search and also at that juncture rescoring the results with additional function can have superior result. One of the best illustrations

to that would be obtaining the AutoDock output files (created docked orientations) than ranking it again with DSX (Drug Score). [52]

Key operation of docking is managing to discover worthy enough situations to reside the candidate compound inside the enzyme where catalytic activity take place, therefore they are fetched together to discover the top matching geometric situation. Ligand molecule angles are accomplished by an algorithm one step at a time and expectantly some positions (situation) of ligands can be located inside the catalytic part of the enzyme. Decision of settlement is accomplished by computing the energy of the system, which uses the molecular mechanics force fields. As the energy gets lower, the better enzyme - compound binding[51,53-55] happens. Entire probable spatial orientations of enzyme - compound complex are conducted by using search algorithm. In our experiment, ligand was assumed as flexible however enzyme was assumed as rigid. Setting ligand as having flexible structure means that it has millions of possible conformations to reach to the lowest energy level due to bargaining rotatable bonds in its structure. Physical interrelation is detected for the candidate compound as well as for the enzyme.

3.2 Preparation of Enzymes and Ligands

Protein Data Bank (PDB) is the main foundation web site to adopt the crystal structures of the two COX enzymes. 1Q4G[56] (Ovine Prostaglandin H2 Synthase-1 (COX-1), in complex with Alpha-Methyl-4-Biphenylacetic, resolution 2.00 Å) and 3NT1[16] (Mus musculusCOX-2 in complex with naproxen, resolution 1.73Å) are the crystal structures that are used. Each structure was cleaned of all water molecules and inhibitors as well as all non-interacting ions before being used in the docking

studies. When inhibitor was bound to the COX enzyme, oxidized form of heme group was used, as adding $^{+2}$ charge to the Fe atom. For COX-1 and COX-2, one of the two subunits was taken as the target structure. Using a fast Dreiding-like force field, each protein's geometry was first optimized and then given in to the "Clean Geometry" toolkit of Discovery Studio (Accelerys Inc.) for a more methodical check. Missing hydrogen atoms were added based on the protonation state of the titratable residues at a pH of 7.4. Ionic strength set was 0.145 and the dielectric constant set was the 10. Then and there the enzyme was minimized and the files were saved as tolerated type, which is necessary for the following docking procedures[44,45].

Candidate compound generation and preparation is the most essential phase in this thesis. Initial point for this operation was based on the structure of the active site cavities of COX-1 and COX-2. The scaffolds generation and building up[44] were achieved by using the module of the commercial software Accelrys' program. The GOLD[55] and AutoDock 4.2[54], Auto-Dock Tools (ADT) programs were used for molecular docking into the active site of COX-1 and COX-2 isozymes and to identify the inhibition constants. Celecoxib used in this study, which has a structural similarity to our resultant scaffolds, was used as a scaffold due to being the most effective and least side effect compound known.

Python script required for separating one ".*sd" file into many "*.pdb" or "*.mol2" files. This is achieved via o'babel[57] program with following script:

babel -m –isd*.sd - *.mol2

3.3 Selecting a Docking Method for Virtual Screening

Other docking programs and scores were used to decide which one gives the fastest result as well as the most accurate result. For further check, AutoDock 4, GoldScore, ChemScore, CHEMPLP and ASP were examined with well-known and currently used inhibitors. Virtual screening returns to false positive and also false negative iterations. In other words, usage of whichever screening algorithm can yield overlooking of a result, which gives one of the efficient compounds or may grab an unusable compound as a drug candidate. Therefore, choosing and picking the suitable scoring function for a purpose and modification into the required condition is significant.

Nearly 10 different drugs are available for well-known COX-2 inhibitor as attest compound, however celecoxib is one of the highly selective ligands that is already available in market; consequently using it as a reference docking is rational. Other docking scores such as ChemScore, CHEMPLP and AutoDock also adapted with the currently used and marketed drugs against COX-2 and their inhibition constants and docking scores were known. Another crucial feature for virtual screening as a second most important point is time consumption; screening should have a high speed since thousands of compounds are tested along accordingly CHEMPLP was chosen to do the screening.

3.4 Docking Based Virtual Screening with CHEMPLP

GOLD (Genetic Optimization for Ligand Docking) is a greatly automated docking tool that allows for optimization and flexible docking with different genetic algorithms[58,59]. The scoring function ranks the dockings according to total score of

energies; hydrogen bond, pairwise dispersion potential that can define a noteworthy impact to hydrophobicity of binding and a molecular mechanism in terms of interior energy of the ligand binding sides[55,60].

CHEMPLP is the greatest scoring function among other scoring functions of GOLD docking software and it is well suited with AutoDock result. For GOLD docking; first of all H atoms are added to enzyme, ligands, then default parameters are used, and cavity detection was disabled since we specify coordinates. A sphere which has 16 Å radius drawn with specific coordinates (for COX-1, x: 26.108 y: 35.061 z: 197.448 and COX-2, x: -39.746, y: -50.781, z: -22.645) is used.

Docking of 1129 candidate compounds into two COX isoenzymes has been conducted concurrently. Calculations take approximately 10 days at least 75% usage of single core per enzyme on High Performance Cluster (HPC) cluster.

GOLD software creates a file named as: bestrankings.lst file that contains score values per ligand. Some columns of this file are transferred to a Microsoft Excel® file. According to formula, it is sorted by using the discrimination values. Discrimination value defines at least 15% alteration between COX-1 and COX-2 dockings scores per ligand. Scores are arranged based on COX-2/COX-1 score ratio. If ratio is lower than 1.15, the candidate compound is considered as non-selective and eliminated. The best 51 ligands from this discriminated and arranged list are shown in Table 4.1. CHEMPLP cannot be the only score used for this study, since the results are supported/confirmed with other scoring functions.

3.5 Validating CHEMPLP Results with Other Docking Tools

Additional GOLD scoring functions such as GoldSscore, ChemScore and ASP work in a computerized manner just like ChemPLP scoring function. Putative parameter group and identical active site coordinate usage directed us to retrieve results one by one because AutoDock does not allow automated docking. For each docking, one has to apply method as the number of ligand and this is time consuming. Specifically Raccoon[61] is a handy script which greatly needs to MGL Tools and it can be used on Portable Batch System (PBS) based HPC clusters nevertheless it encounters various problems such as needing other programs. Necessity of classy tool for conducting AutoDock experiments in parallel, a novel tool was built in order to overcome this problem. This novel tool is called YaVST[62] (Yet Another Virtual Screening Tool), created by our colleague, Serkan Altuntaş. YaVST is a free access, open-source software and used for virtual screening via AutoDock 4 (Website for YaVST is: https://github.com/serkanaltuntas/yavst). Similar to its prototypes, it is also heavily interrelated to MGL which is a software developed at the Molecular Graphics Laboratory (MGL) of The Scripps Research Institute for visualization and analysis of molecular structures Tools , but it is settled as a self-contained package so it does not necessitate MGL Tools.

YaVST generates workspaces automatically for each run. For this study, each workspace contains vast amount of ligands per enzyme.

If not available, YaVST generates the PDBQT files from PDB file for each ligand. After that, creation of a Docking Parameter Files (DPF) and one single Grid

Parameter File (GPF) for each ligand keep track of that step. Scripts of MGL Tools create these output files consequently; it generates the same output that is identical to AutoDockTools.

Besides pdbqt, gpf and dpf files, YaVST generates several qsub files that are needed for job submission to any type of Sun Grid Engine based HPC. Eventually as it happens in manual docking, each experiment generates .dlg file and with a small script, .pdb file of the lowest energy result retrieved from .dlg file and list of the lowest energy and Ki values, which stands for the dissociation constant of an enzyme-inhibitor complex, were extracted from each .dlg file. This is a very effective way of conducting Autodock 4 experiments without spending much time.

3.6. ADMET

Not obtaining a promising ADMET feature, which stands for the Absorption, Distribution, Metabolism, Excretion, and Toxicity characteristics of a candidate compound headed for organism, is one of the utmost discouraging obstacles for drug development. Any drug must contain all these characteristics to be used in clinical trials. This enables us to do the early optimization. The dispositions of the candidate compound used by the organism were controlled with ADMET PSA 2D (polar surface area) against ADMET AlogP98 (the logarithm of the partition coefficient between *n*-octanol and water). If the candidate compound cannot pass ADMET test, progressive steps might become loss of time. Determination of which compound can pass ADMET and removal of undesirable compounds make the research course more cost operative and effective[63].

4. Chapter 4: Results and Discussion

4.1 Docking Results

In total 1129 *de novo* potential COX-2 inhibitor ligands were designed via Accelerys. All ligands were simultaneously docked via GOLD and AutoDock program. 66 were eliminated according to AutoDock results, which are positive value for free energy for either COX-1 or COX-2. Having a positive sign score of free energy for a ligand means that; K_i values could not be calculated since they are unfavorable for either COX-1 or COX-2 and cannot give result of COX-2/COX-1 ratio and it is unusable. After obtaining results, the best 53 *de novo* designed COX-2 inhibitors were determined according to the total score of ChemPLP, ChemScore and ASP which are 1.15 fold and above for the ligands compared to COX-1, as well as for AutoDock 4, 1.15..Table-4.1 shows score results of GOLD (including GoldScore and AutoDock 4 Free energy and K_i values) for each ligand. According to this elimination, SC_558 and celecoxib were in highly selected ligand list; but in order to find new drugs these 2 were eliminated and the rest51 are listed in Table 4.1.

To find better and highly selective Cox-2 inhibitor than inhibitors found currently in the market, Aspirin, ketoprofen, ketorolac, celecoxib, etodolac, lumiracoxib, rofecoxib, sc_558 and nimesulide were used as a control in a simultaneously run docking to discuss program's validity.. Score values for each drug is given in Table 4.2.

Table 4. 1: Docking scores of each candidate retrieved from GOLD; K_i and Free energy (kcal/mol) values retrieved from AutoDock 4

Molecule	ChemPLP		ASP		ChemScore		GoldScore		AutoDock4(kcal/mol)		AutoDock4(K_i)			
	COX-1	COX-2	COX-1	COX-2	COX-1	COX-2	COX-1	COX-2	COX-1	COX-2	COX-1		COX-2	
TM_01	**16,43**	**101,04**	**-0,13**	**41,69**	**41,08**	**59,67**	**-100,67**	**34,81**	**-2,64**	**-14,82**	**11,55**	**mM**	**13,79**	**pM**
TM_02	**14,57**	**109,17**	**2,63**	**38,05**	**43,08**	**57,69**	**-90,57**	**75,8**	**-3,98**	**-12,52**	**1,21**	**mM**	**662,85**	**pM**
TM_03	16,47	84,97	-1,33	36,56	43,34	54,62	-89,89	32,57	-8,67	-13,97	438,07	nM	57,98	pM
TM_04	**30,01**	**105,67**	**10,04**	**40,52**	**41,56**	**57,21**	**-42,07**	**75**	**-0,85**	**-13,87**	**238**	**mM**	**67,58**	**pM**
TM_05	25,77	102,36	15,58	42,75	45,91	61,39	-26,92	75,35	-3,65	-14,03	2,11	mM	51,86	pM
TM_06	26,22	107,69	21,24	44,98	41,48	56,22	-4,28	80,59	-3,63	-12,72	2,2	mM	475,46	pM
TM_07	**28,89**	**104,04**	**16,27**	**40,2**	**41,63**	**57,18**	**-44,28**	**75,02**	**-1,87**	**-13,35**	**42,6**	**mM**	**164,57**	**pM**
TM_08	34,01	105,1	18,88	46,36	38,15	50,57	-1,59	76,66	-2,29	-14,25	20,82	mM	35,84	pM
TM_09	**26,36**	**93,16**	**16,28**	**40,08**	**44,33**	**57,6**	**-29,45**	**66,81**	**-1,08**	**-12,96**	**161,81**	**mM**	**314,51**	**pM**
TM_10	31,7	103,71	12,67	39,01	46,21	53,77	24,11	67,01	-0,43	-10,46	483,48	mM	21,51	nM
TM_11	34,34	102,66	17,1	46,06	44,17	58,21	-0,17	82,13	-4,71	-12,81	354,46	uM	405,68	pM
TM_12	**32,99**	**100,06**	**19,27**	**44,24**	**41,49**	**56,08**	**6,17**	**75,69**	**-0,14**	**-9,34**	**783,84**	**mM**	**142,94**	**nM**
TM_13	34,15	100,47	15,42	40,94	44,75	59,56	-25,3	65,91	-0,45	-11,96	468,27	mM	1,72	nM
TM_14	36,93	112,89	18,05	42,37	44,68	55,33	-10,44	81,73	-7,35	-14,84	4,06	uM	13,22	pM
TM_15	27,97	91,48	17,82	39,82	42,78	54,29	-14,95	65,27	-1,26	-11,48	119,72	mM	3,86	nM
TM_16	**32,1**	**102,66**	**18,36**	**40,24**	**44,31**	**54,24**	**18,84**	**83,66**	**-0,33**	**-13,23**	**574,52**	**mM**	**198,97**	**pM**
TM_17	31,39	100,37	20	43,74	45,59	57,32	-74,53	78,17	-3,09	-11,49	5,4	mM	3,77	nM
TM_18	**32,43**	**105,76**	**22,11**	**43,9**	**47,33**	**58,87**	**-51,3**	**74,3**	**-1,82**	**-13,67**	**46,09**	**mM**	**95,03**	**pM**
TM_19	36,29	97,85	16,56	39,44	41,29	54,52	11,55	74,88	-2,86	-12,29	7,98	mM	982,62	pM
TM_20	37,81	98,69	14,97	42,51	44,86	56,41	-19,66	51,54	-2,85	-14,07	8,1	mM	48,75	pM
TM_21	40,82	98,4	17	41,2	38,33	53,03	14,09	73,88	-2,93	-12,69	7,1	mM	500,05	pM
TM_22	34,12	105,1	24,08	44,23	45,19	57,05	6,26	72,11	-2,06	-13,05	30,97	mM	269,58	pM
TM_23	35,21	99,41	22,24	42,09	38,46	49,15	8,48	74,99	-1,06	-11,45	166,29	mM	4,04	nM
TM_24	**33,64**	**101,86**	**22,21**	**41,81**	**44,93**	**54,82**	**-5,58**	**51,21**	**-0,29**	**-13,87**	**610,5**	**mM**	**68,39**	**pM**
TM_25	35,74	98,05	21,04	40,6	44,66	59,36	24,73	79,79	-4,83	-12,48	286,11	uM	715,72	pM

Molecule	ChemPLP		ASP		ChemScore		GoldScore		AutoDock4(kcal/mol)		AutoDock4(Ki)			
	COX-1	COX-2	COX-1	COX-2	COX-1	COX-2	COX-1	COX-2	COX-1	COX-2	COX-1		COX-2	
TM_26	34,59	89,41	19,68	44,84	46,13	60,7	-18,4	37,56	-2,94	-13,75	7,05	mM	84,01	pM
TM_27	**42,92**	**107,54**	**19,21**	**44,66**	**47,24**	**59,49**	**21,98**	**73,39**	**-0,82**	**-13,31**	**248,87**	**mM**	**175,25**	**pM**
TM_28	**43,18**	**106,3**	**21,01**	**45,14**	**44,9**	**57,74**	**-12,8**	**65,7**	**-2,13**	**-13,88**	**27,44**	**mM**	**66,58**	**pM**
TM_29	37,77	102,16	20,69	44,99	48,69	57,82	-10,09	50,85	-2,58	-13,61	12,78	mM	105,59	pM
TM_30	41,38	99,57	21,45	41,65	45,02	57,12	-16,82	34,86	-0,89	-12,03	223,76	mM	1,52	nM
TM_31	**42**	**96,54**	**17,08**	**38,39**	**46,26**	**53,43**	**-36,44**	**72,69**	**-0,51**	**-12,53**	**420,36**	**mM**	**653,39**	**pM**
TM_32	39,21	89,25	15,44	25,95	41,64	51,8	-46,22	56,2	-5,35	-12,19	119,38	uM	1,15	nM
TM_33	44,57	79,57	20,44	34,46	33,33	48,76	9,27	44,45	-5,82	-9,9	53,88	uM	55,16	nM
TM_34	**43,84**	**78,67**	**30,73**	**43,85**	**38,28**	**52,58**	**0**	**52,2**	**-1,42**	**-8,69**	**91,02**	**mM**	**429,15**	**nM**
TM_35	37,96	75,69	26,69	32,3	36,79	46,37	18,34	42,95	-6,19	-9,76	29,04	uM	69,61	nM
TM_36	43,13	84,69	37,88	42,99	33,79	44,39	0	0	-2,84	-10,85	8,33	mM	11,15	nM
TM_37	53,13	80,55	39,92	54,67	43,43	51,51	0	14,65	-2,28	-6,54	21,16	mM	15,96	uM
TM_38	47,25	72,93	27,58	32,47	36,86	44,72	28,2	37,99	-7,84	-9,08	1,8	uM	222,37	nM
TM_39	**77,66**	**97,73**	**15,76**	**38,01**	**46,33**	**51,41**	**25,65**	**51,84**	**-3,26**	**-9,59**	**4,07**	**mM**	**93,36**	**nM**
TM_40	30,3	53,64	5,95	7,86	43,95	42,61	0	0	-0,79	-8,04	262,11	mM	1,28	uM
TM_41	65,5	84,48	49,52	52,35	42,51	54,88	88,49	81,13	-12,81	-14,64	404,47	pM	18,42	pM
TM_42	64,17	79,92	25,55	33,73	42,12	45,05	48,85	60,36	-8,39	-9,96	704,53	nM	50,31	nM
TM_43	69,24	85,76	27,74	40,02	50,55	49,61	40,83	73,11	-7,39	-8,97	3,84	uM	266,68	nM
TM_44	64,98	80,2	27,05	33,51	42,42	45,06	47,89	59,98	-8,59	-9,96	503,62	nM	49,85	nM
TM_45	60,29	86,91	41,39	35,27	44,81	50,37	68,91	77,66	-11,43	-13,3	4,15	nM	176,83	pM
TM_46	78,48	102,55	29,85	33,35	50,57	50,99	70,88	59,12	-8,18	-12,95	1,01	uM	321,73	pM
TM_47	88,42	98,31	38,2	43,3	34,07	47,38	0	59,3	-5,41	-10,58	107,55	uM	17,45	nM
TM_48	57,52	75,76	33,82	37,26	40,22	41,15	51,25	64,9	-6,7	-8,66	12,22	uM	450,88	nM
TM_49	**65,24**	**81,14**	**30,08**	**35,21**	**40,92**	**42,97**	**2,6**	**61,41**	**-1,16**	**-11,57**	**140,92**	**mM**	**3,31**	**nM**
TM_50	74,92	96,42	42,1	38,04	45,62	55,1	71,64	82,37	-10,31	-12,25	27,77	nM	1,05	nM
TM_51	81,33	97,15	43,48	39,06	46,22	60,82	84,73	79,38	-11,47	-13,97	3,89	nM	57,83	pM

Table 4. 2: Scores of known COX-1 or COX-2 inhibitors. Selective drugs are marked with bold.

Molecule	ChemPLP		ASP		ChemScore		GoldScore		AutoDock 4 (kcal/mol)		AutoDock 4 (Ki)			
	COX-1	COX-2	COX-1	COX-2	COX-1	COX-2	COX-1	COX-2	COX-1	COX-2	COX-1		COX-2	
Aspirin	33,55	34,9	19,48	17,39	16,5	16,01	41,32	38,69	-5,53	-5,54	87,87	uM	86,25	uM
Ketoprofen	38,66	39,06	18,86	16,61	18,63	19,41	31,17	34,35	-9,02	-8,89	243	nM	302,58	nM
Ketorolac	45,28	46,59	24,47	19,15	22,74	23,5	34,4	42,43	-8,84	-8,3	328,64	nM	824,68	nM
Celecoxib	39,93	58,01	28,48	28,01	23,16	26,34	41,15	46,81	-8,4	-10,46	696,68	nM	21,57	nM
Etodolac	34,79	45,08	21,93	18,12	22,71	23,96	38,31	47,86	-7,73	-9,11	2,15	uM	209,85	nM
Lumiracoxib	43,86	43,91	24,69	20,79	20,8	19,69	34,01	33,58	-6,92	-7,72	8,45	uM	2,18	uM
Rofecoxib	40,88	44,69	20,04	20,03	28,4	28,3	41,06	43,78	-9,99	-10,1	47,63	nM	39,34	nM
SC_558	40,03	58,19	28,7	31,85	24,86	28,89	38,59	51,96	-8,63	-10,66	473,2	nM	15,27	nM
Nimesulide	39,17	41,22	25,27	24,66	18,94	20,53	34,53	40,66	-7,76	-8,5	2,05	uM	592,4	nM

Table 4. 3: Folds of ratios calculated from Table 4.2 and resulting COX-2/1 inhibitor case

	GOLD COX-2/COX-1	AUTODOCK COX-2/COX-1 (kcal/mol)	AutoDock 4 (Ki)				AUTODOCK COX-2/COX-1 (K$_i$)	GOLD COX-2/COX-1	AUTODOCK COX-2/COX-1
			COX-1		COX-2				
Aspirin	0,98	1,00	87,87	uM	86,25	uM	0,98	COX-1	COX-2
Ketoprofen	0,99	0,99	243	nM	302,58	nM	1,25	COX-1	COX-1
Ketorolac	0,96	0,94	328,64	nM	824,68	nM	2,51	COX-1	COX-1
Celecoxib	1,23	1,25	696,68	nM	21,57	nM	0,03	COX-2	COX-2
Etodolac	1,10	1,18	2,15	uM	209,85	nM	0,10	COX-2	COX-2
Lumiracoxib	0,94	1,12	8,45	uM	2,18	uM	0,26	COX-1	COX-2
Rofecoxib	1,04	1,01	47,63	nM	39,34	nM	0,83	COX-2	COX-2
SC_558	1,27	1,24	473,2	nM	15,27	nM	0,03	COX-2	COX-2
Nimesulide	1,04	1,10	2,05	uM	592,4	nM	0,29	COX-2	COX-2

Celecoxib is the drug, which is used for inhibiting COX-2 and can be found currently in the market; however, it has many long term use side effect.

Elimination of ligands with COX-2/COX-1 inhibition ratio, in order to study in more detail, celecoxib scores were taken as a baseline. Ligands with better scores than celecoxib are highlighted in Table 4.1. In the following Table 4.4, COX-2 GOLD score folds against COX-1, COX-2 AutoDock 4 free energy folds against COX-1 and COX-2 ChemPLP scores against COX-1 retrieved from GOLD were collected. 13 COX-2 targeted *de novo* designed ligands were found, namely; TM_01, TM_02, TM_04, TM_07, TM_09, TM_12, TM_16, TM_18, TM_24, TM_27, TM_28, TM_31, TM_34. Their COX-2/COX-1 inhibition ratios are higher than any other known COX-2 selective inhibitors, according to calculation by ChemPLP, AutoDock and Gold.

Table 4. 4: COX-2 based designed drug's folds

Molecule	GOLD COX-2/COX-1	AutoDock4 (kcal/mol) COX-2/COX-1	AutoDock4 (K_i) COX-2/COX-1	ChemPLP COX-2/COX-1
TM_01	3,53	5,61	1,19E-09	6,15
TM_02	3,40	3,15	5,48E-07	7,49
TM_04	2,49	16,32	2,84E-10	3,52
TM_07	2,32	7,14	3,86E-09	3,60
TM_09	2,19	12,00	1,94E-09	3,53
TM_12	2,14	66,71	1,82E-07	3,03
TM_16	2,08	40,09	3,46E-10	3,20
TM_18	2,05	7,51	2,06E-09	3,26
TM_24	1,97	47,83	1,12E-10	3,03
TM_27	1,94	16,23	7,04E-10	2,51
TM_28	1,92	6,52	2,43E-09	2,46
TM_31	1,79	24,57	1,55E-09	2,30
TM_34	1,55	6,12	4,71E-06	1,79
TM_39	1,34	2,94	2,29E-05	1,26
TM_49	1,17	9,97	2,35E-08	1,24

From another perspective, COX-1 *de novo* ligands were designed to inhibit COX-1. However, here failed COX-1 based *de novo* ligands were docked into COX-2. 23 ligands in Table 4.5 have 1.15 fold and above ratio of COX-2/COX-1. After further elimination, scores were compared to celecoxib and SC_558, eventually 6 ligands remained. However, surprisingly only TM_v_20 has the best fold among all. Therefore, only TM_v_20 was selected from this group since its ChemPLP, AutoDock and Gold folds are higher than any other known COX-2 selective inhibitors. Ratios are compared to values listed in Table 4.7 since it contains known inhibitor score values retrieved from GOLD and AutoDock 4.

Table 4. 5: COX-1 based *de novo* designed drug scores

Molecule	ChemPLP		ASP		ChemScore		GoldScore		AutoDock 4 (kcal/mol)		AutoDock 4 (Ki)			
	COX-1	COX-2	COX-1	COX-2	COX-1	COX-2	COX-1	COX-2	COX-1	COX-2	COX-1		COX-2	
TM_v_01	66,50	96,59	36,24	47,95	33,02	43,94	11,99	74,17	-2,21	-8,21	23,97	mM	961,68	nM
TM_v_02	71,54	92,92	32,73	53,30	34,78	39,46	21,15	61,45	-3,24	-10,88	4,25	mM	10,54	nM
TM_v_03	62,94	77,48	47,41	47,78	37,58	44,38	-0,66	66,54	-4,19	-10,98	850,42	uM	8,93	nM
TM_v_04	82,79	91,97	39,83	49,84	38,43	45,57	10,40	66,46	-3,83	-9,51	1,55	mM	106,04	nM
TM_v_05	53,65	91,09	35,13	36,78	38,02	40,22	18,28	60,90	-5,33	-10,62	123,04	uM	16,52	nM
TM_v_06	66,99	89,78	32,95	32,72	39,72	46,73	51,15	63,73	-5,22	-9,96	149,06	uM	49,72	nM
TM_v_07	43,29	52,28	19,35	28,18	30,12	32,82	-45,74	43,53	-5,70	-10,56	66,13	uM	18,32	nM
TM_v_08	52,43	80,96	42,68	53,79	36,22	41,81	0,00	65,54	-5,28	-9,24	135,27	uM	167,43	nM
TM_v_09	71,80	83,38	38,94	48,45	38,16	41,94	8,71	74,14	-6,68	-10,70	12,67	uM	14,30	nM
TM_v_10	48,72	69,66	36,22	33,42	29,60	29,97	44,99	67,38	-6,16	-9,34	30,70	uM	141,99	nM
TM_v_11	78,10	97,36	48,29	51,84	35,96	38,19	34,64	63,65	-6,41	-9,68	20,18	uM	80,30	nM
TM_v_12	67,13	82,66	34,45	46,90	35,18	38,46	-0,78	69,11	-6,44	-9,54	19,01	uM	101,32	nM
TM_v_13	60,78	77,05	34,80	45,46	41,51	41,86	17,02	64,06	-7,47	-10,82	3,32	uM	11,81	nM
TM_v_14	62,00	89,38	35,44	44,72	34,02	40,96	32,96	49,95	-7,63	-10,94	2,56	uM	9,64	nM
TM_v_15	58,72	95,19	35,14	38,29	36,84	40,42	33,06	78,48	-7,95	-11,26	1,50	uM	5,56	nM
TM_v_16	70,56	84,32	42,85	50,14	40,03	41,57	49,13	73,21	-6,96	-9,79	7,97	uM	66,68	nM
TM_v_17	54,92	81,67	35,63	40,87	35,38	41,71	25,10	63,25	-6,37	-8,88	21,47	uM	307,97	nM
TM_v_18	73,22	96,13	38,22	53,13	41,02	41,88	8,75	76,17	-9,10	-12,21	214,17	nM	1,12	nM
TM_v_19	62,94	80,41	32,11	36,99	41,58	47,49	40,70	53,73	-7,18	-9,29	5,43	uM	155,78	nM
TM_v_20	**61,06**	**92,71**	**36,43**	**49,48**	**37,26**	**45,34**	**6,72**	**52,56**	**-10,11**	**-12,84**	**38,70**	**nM**	**389,99**	**pM**
TM_v_21	72,04	85,03	37,65	51,46	41,80	39,47	49,10	65,48	-9,57	-12,07	96,34	nM	1,43	nM
TM_v_22	59,63	80,68	40,07	46,82	38,43	39,07	28,09	68,38	-9,32	-11,17	147,59	nM	6,46	nM
TM_v_23	57,07	87,13	35,75	54,45	44,61	55,85	34,70	62,92	-10,56	-12,22	18,07	nM	1,11	nM

Table 4. 6:COX-1 based designed drug's folds

Molecule Name	Total Gold Score of COX-2/COX-1	Autodock4 Energy (kcal/mol) COX-2/COX-1	Autodock4 (Ki) COX-2/COX-1	ChemPLP COX-2/COX-1
TM_v_01	1,39	3,71	4,01E-05	1,45
TM_v_05	1,33	1,99	1,34E-04	1,70
TM_v_08	1,34	1,75	1,24E-03	1,54
TM_v_15	1,33	1,42	3,71E-03	1,62
TM_v_17	1,30	1,39	1,43E-02	1,49
TM_v_20	**1,39**	**1,27**	1,01E-02	**1,52**

Table 4. 7: Fold of Known Drugs

Molecule Name	Total Gold Score of COX2/COX1	Autodock4 Energy (kcal/mol) COX2/COX2	Autodock4 (Ki) COX-2/COX-1	ChemPLP COX2/COX1
SC_558	1,39	1,23	3,37E-02	1,57
Celecoxib	1,28	1,25	2,77E-02	1,49

14 ligands were derived from 3 main scaffold and namely they are; TM_2013_04_07_151011_894 (COX-2 based), TM_2013_05_17_230538_994 (COX-2 based), TM_2013_05_17_231259_735 (COX-1 based). Detailed explanation of elimination and also from which library *de novo* designed drugs originate from is summarized below:
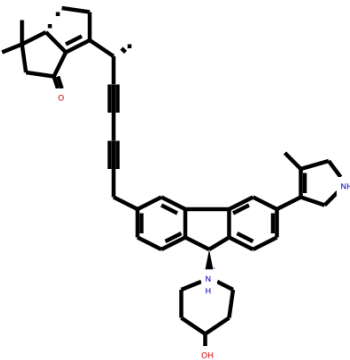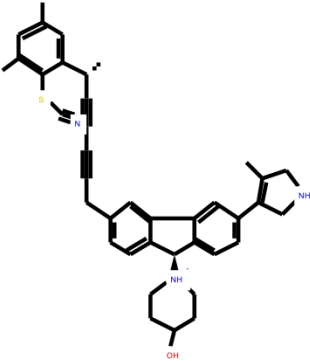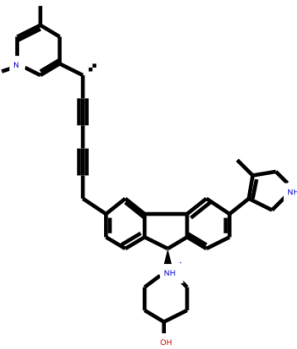
TM_2013_04_07_151011_894 →*de novo* receptor → 1384 fragment was created (instock_lead_21_p1_1) → *de novo* evolution→ 50 ligand (instog_frag_link_1_0) → obabel→ autodock and GOLD → selection
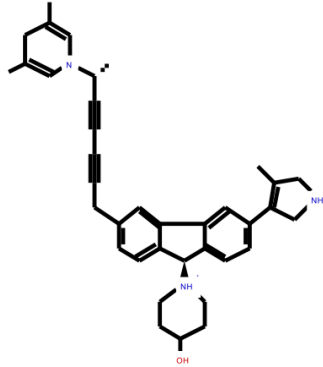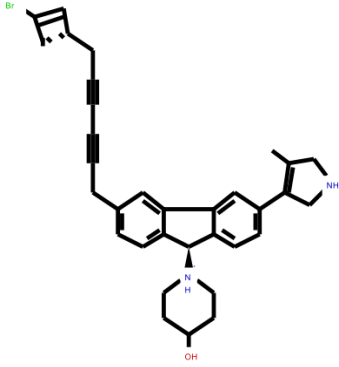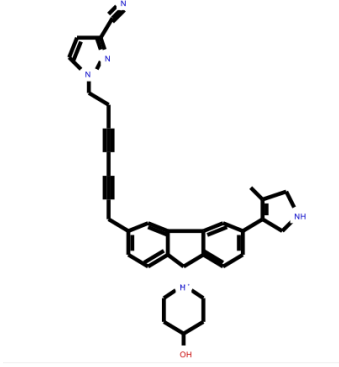
TM_2013_05_17_230538_994 →*de novo* receptor →601 fragment (instock_lead_21_p1_1) → *de novo* evolution → 50 ligand (instog_frag_link_1_0) and 7 ligand (peptide_fragsx) → obabel → autodock and GOLD→selection
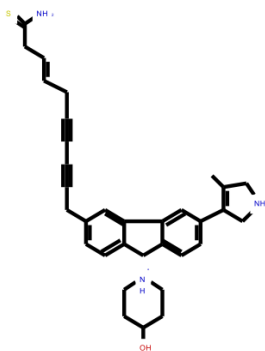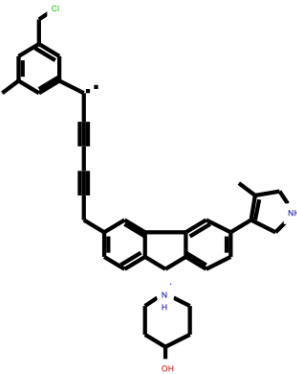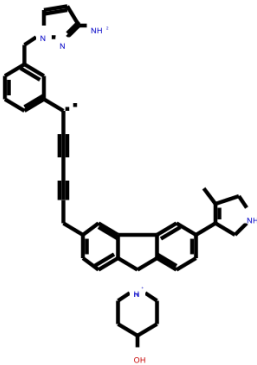
TM_2013_05_17_231259_735 → *de novo* receptor → 3 fragment (instock_lead_21_p1_1) → *de novo* evolution→ 50ligand (instog_frag_link_1_0)and 1 ligand (peptide_fragsx) → obabel→ autodock and GOLD → selection
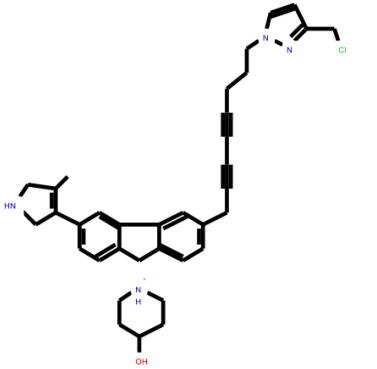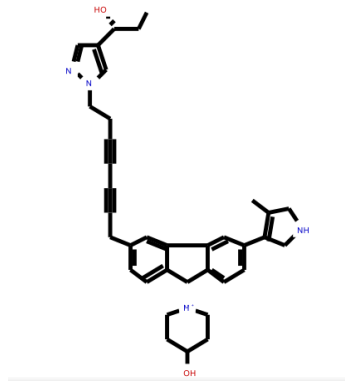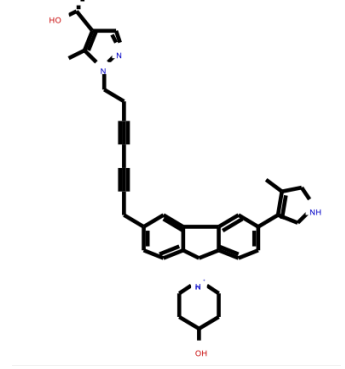
Library names were expressed in parenthesis above.

2-D, 3-D structures, 2-D interaction map and COX-2 enzyme surface around ligand and for the ligands that passed ADMET, interacting residues of COX-2 with ligand can be found in Figure 4.1-4.43.
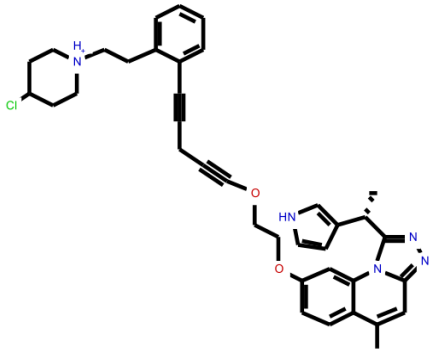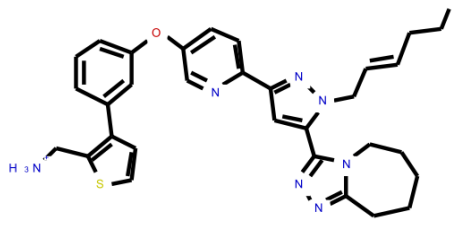
Molecule Open Formula	Molecule Name	Molecular Weight (Da)
	TM_01	**352,9**
	TM_02	**360,75**
	TM_04	**328,17**

	TM_07	**328,17**
	TM_09	**342,52**
	TM_12	**326,93**

	TM_16	**323,35**
	TM_18	**347,11**
	TM_24	**366,75**

	TM_27	**341,06**
	TM_28	**346,86**
	TM_31	**346,86**

	TM_34	**374,22**
	TM_v_20	**341,42**

Figure 4. 1: 2-D Molecule structures of highly selective ligands

For Figure 4.1 - 4.51 each color stands for a specific atom: Red: Oxygen, White: Hydrogen, Yellow: Sulphur, Blue: Nitrogen, Green: Chloride, Black: Carbon, Mahogani: Bromide.
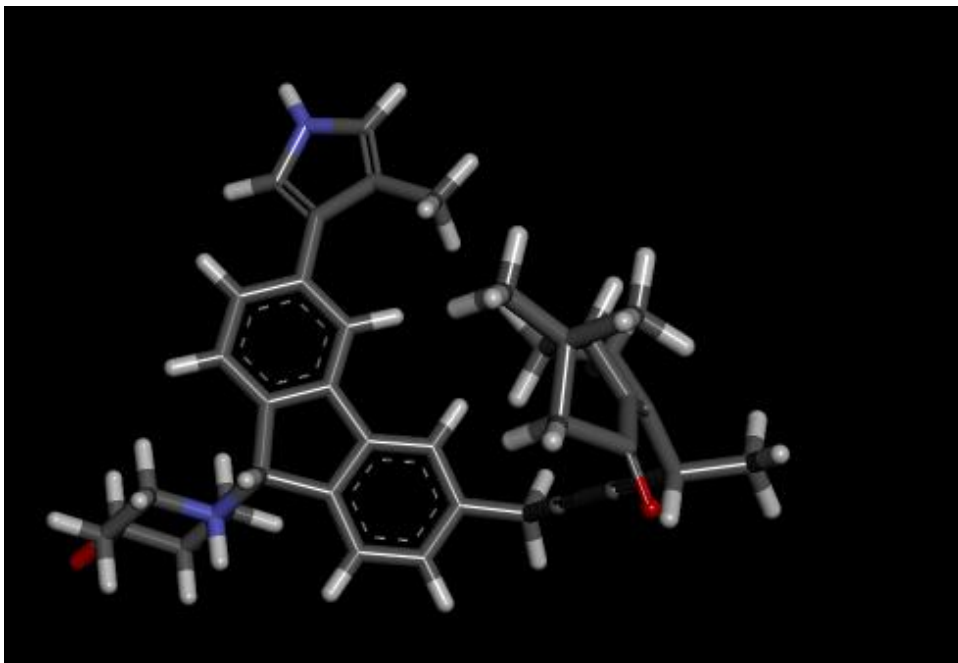
Figure 4. 2: 3-D molecular view of TM_01
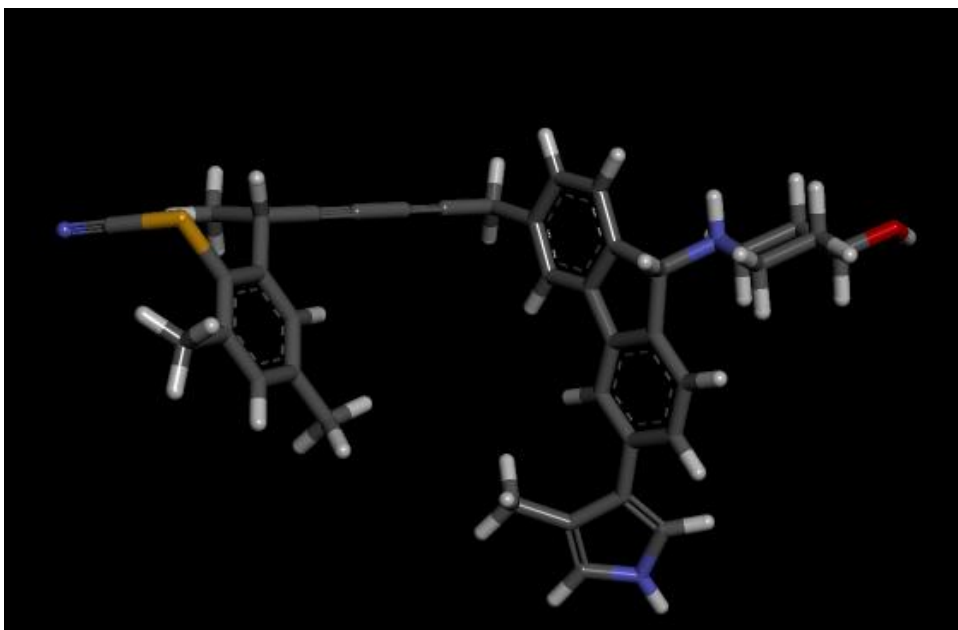
Figure 4. 3: 3-D molecular view of TM_02
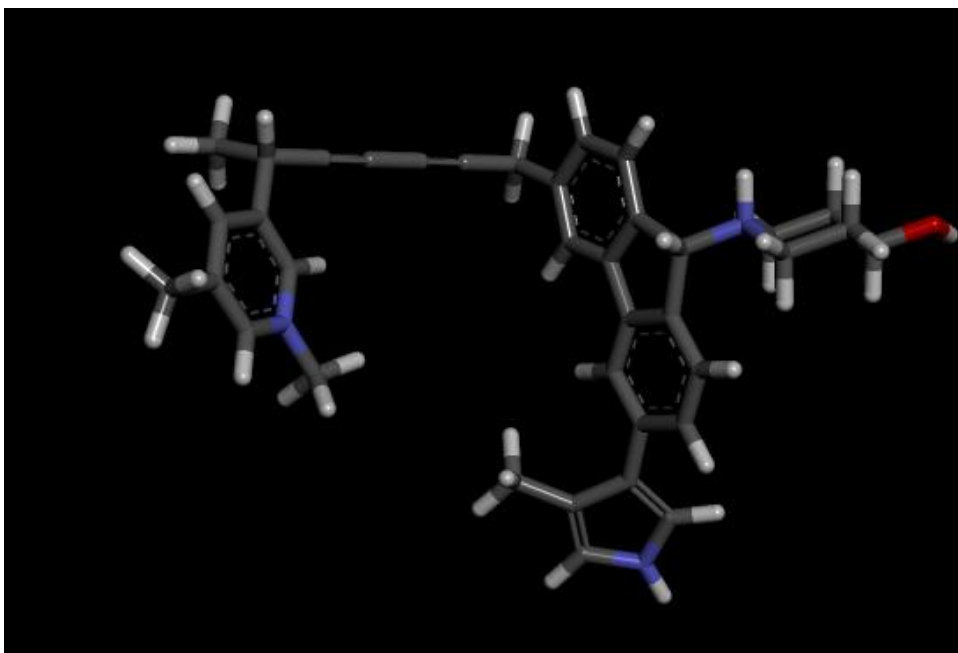
Figure 4. 4: 3-D molecular view of TM_04
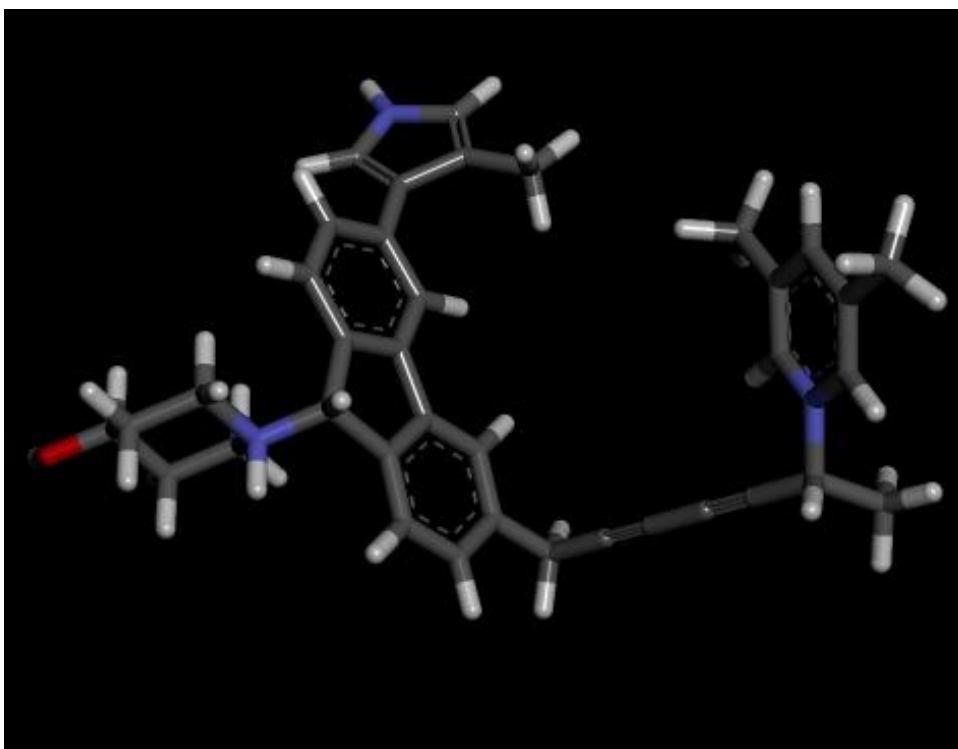
Figure 4. 5: 3-D molecular view of TM_07
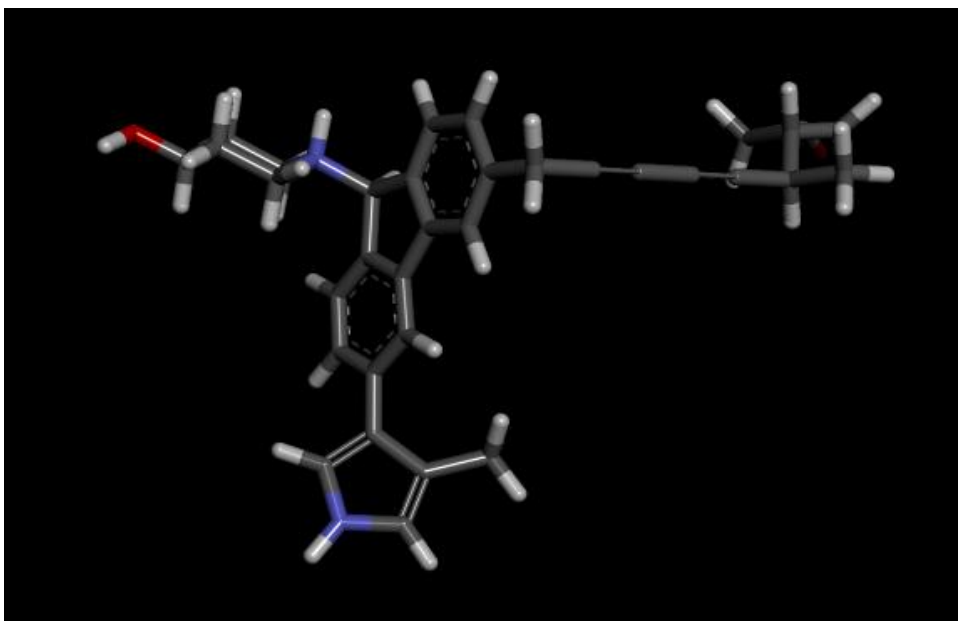
Figure 4. 6: 3-D molecular view of TM_09
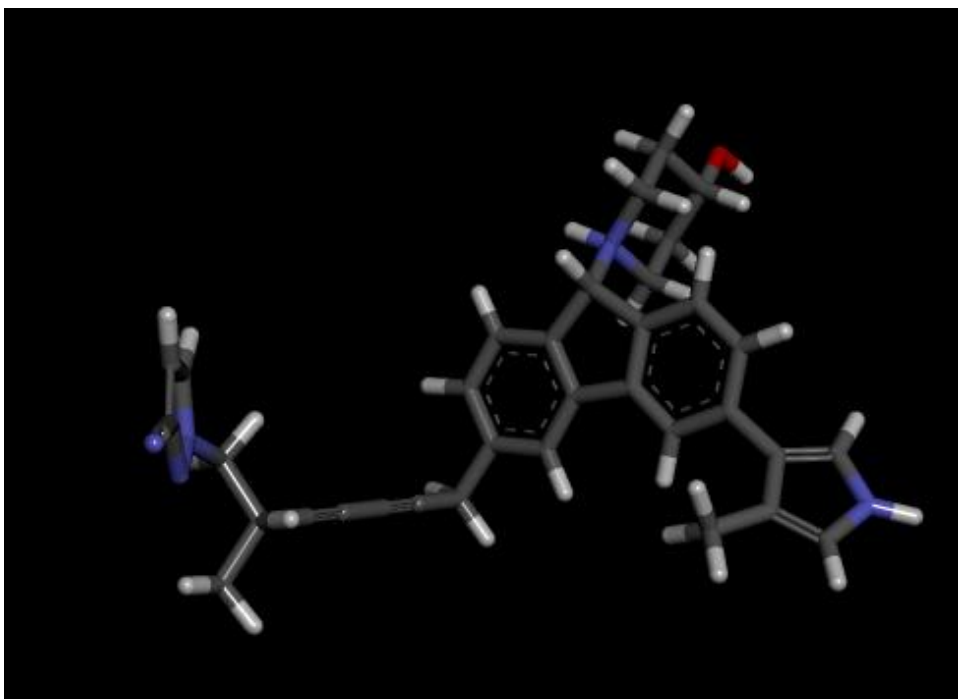
Figure 4. 7: 3-D molecular view of TM_12
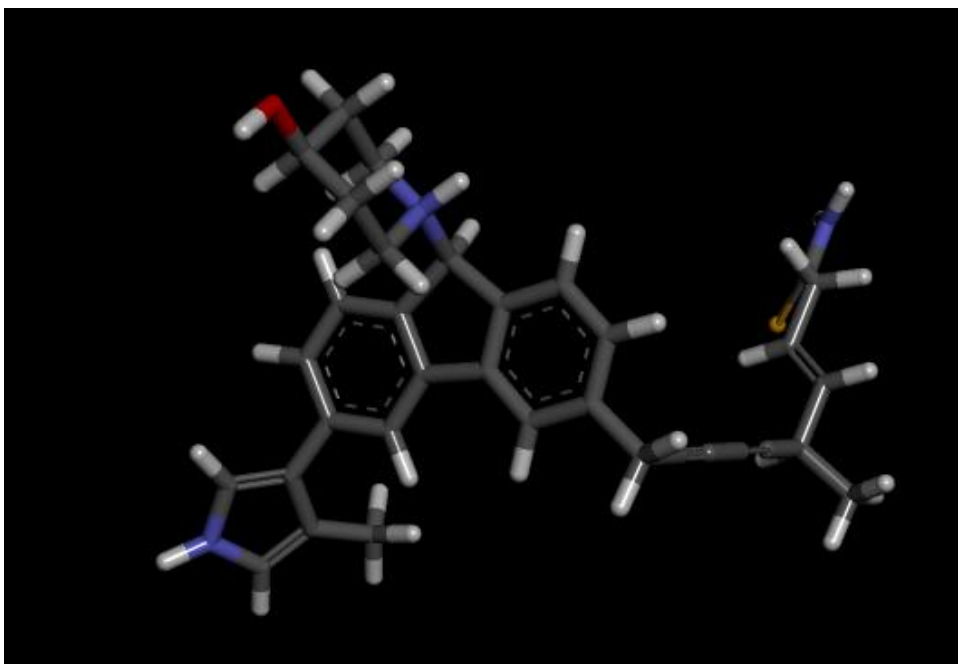
Figure 4. 8: 3-D molecular view of TM_16
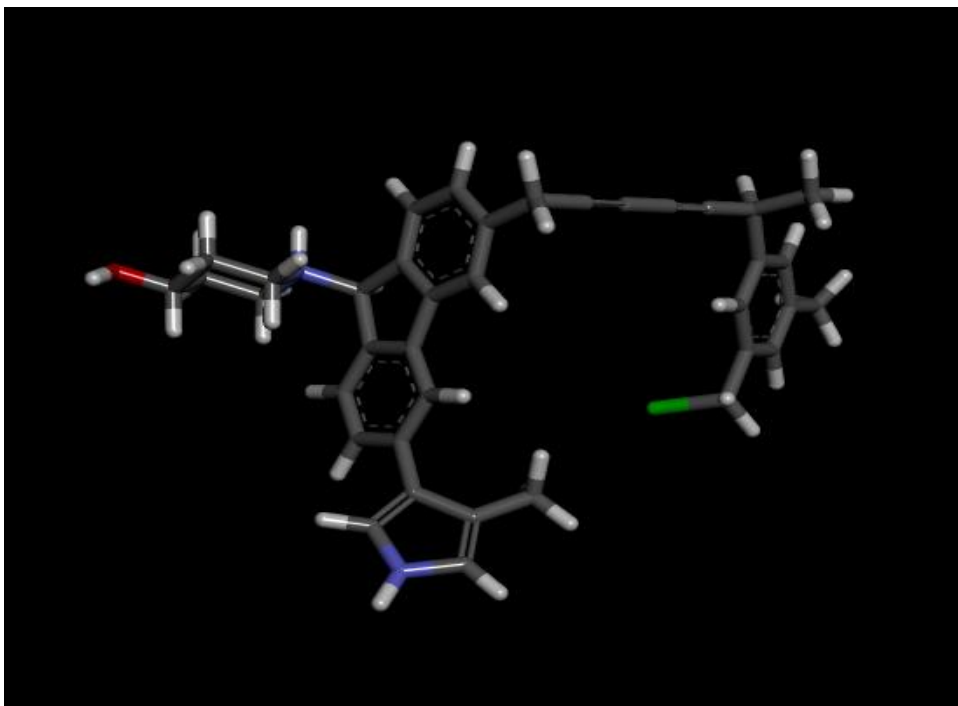
Figure 4. 9: 3-D molecular view of TM_18
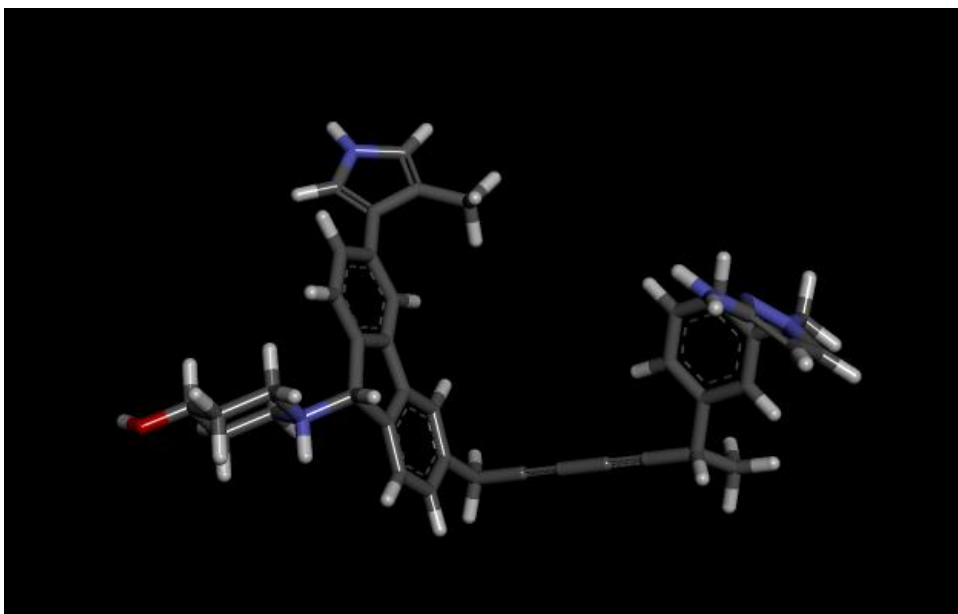
Figure 4. 10: 3-D molecular view of TM_24
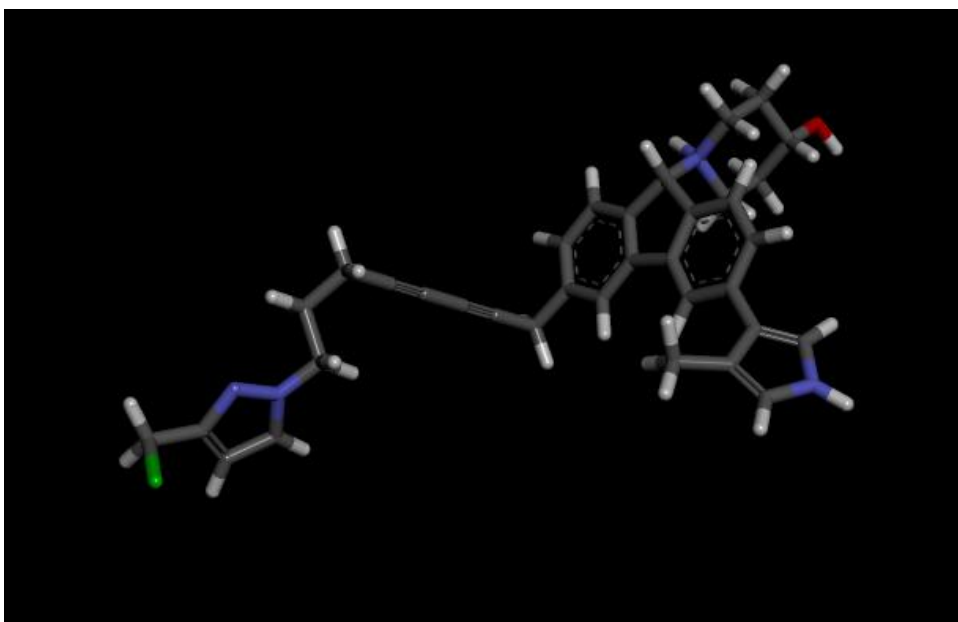
Figure 4. 11: 3-D molecular view of TM_27
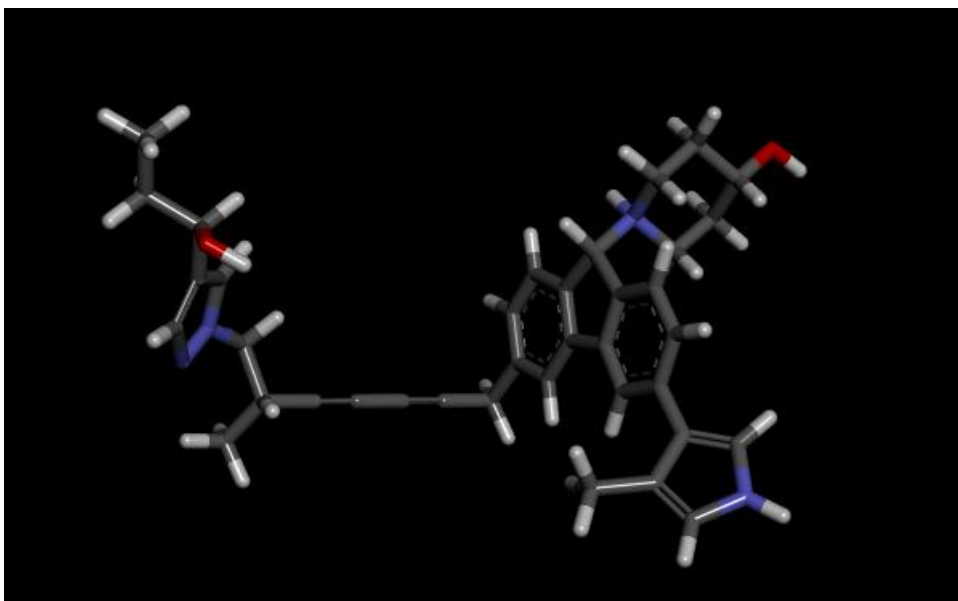
Figure 4. 12: 3-D molecular view of TM_28
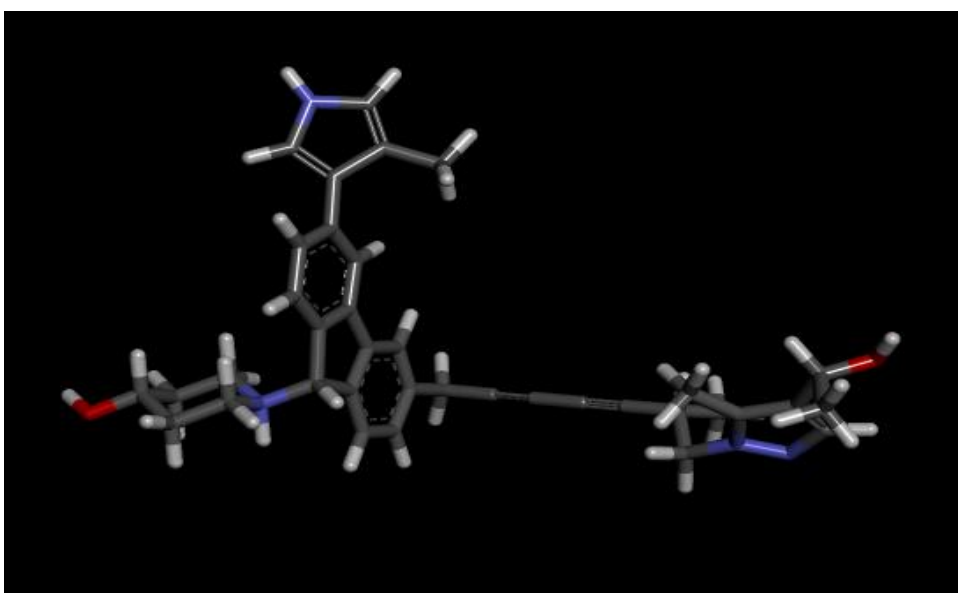
Figure 4. 13: 3-D molecular view of TM_31
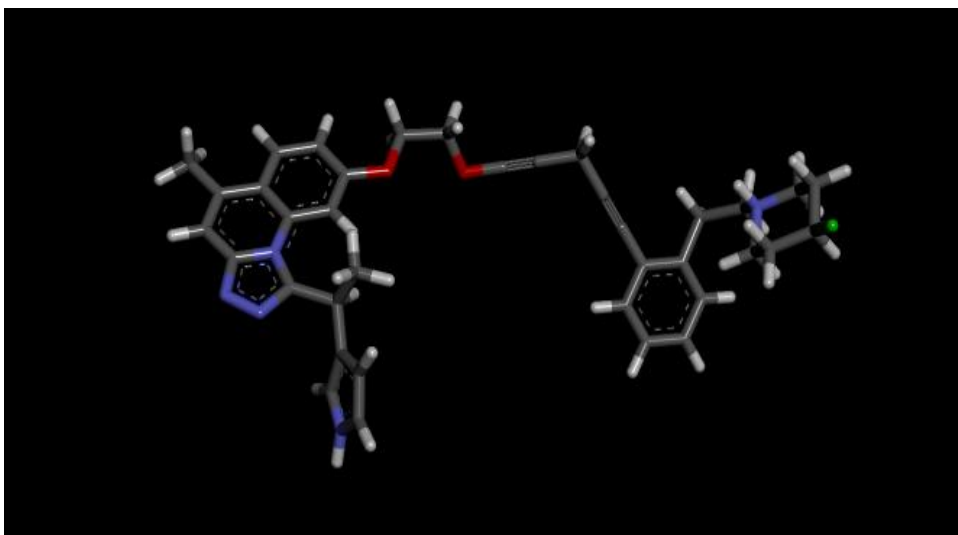
Figure 4. 14: 3-D molecular view of TM_34
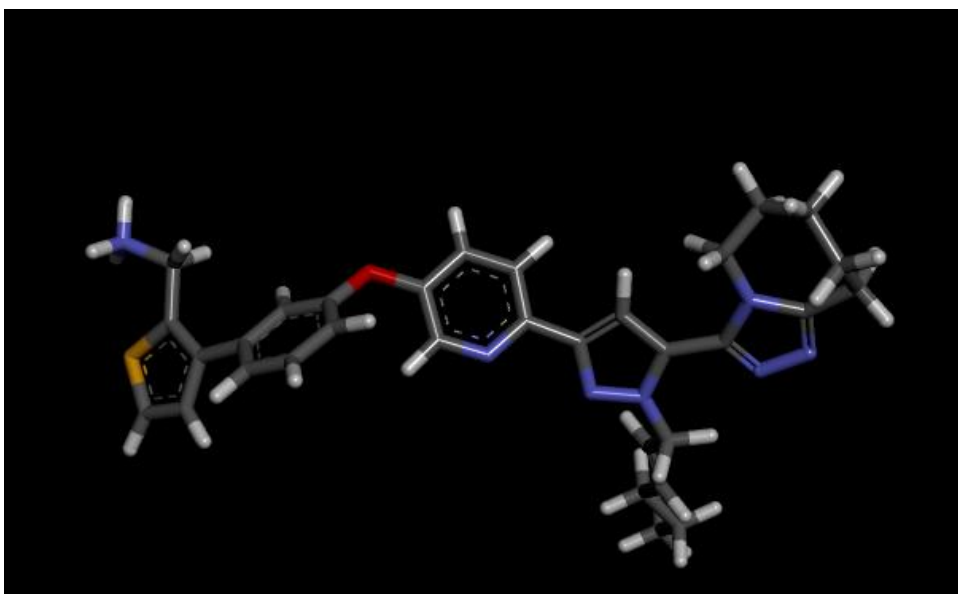
Figure 4. 15: 3-D molecular view of TM_v_20

For 2-D interaction map figures, legend is as follows;
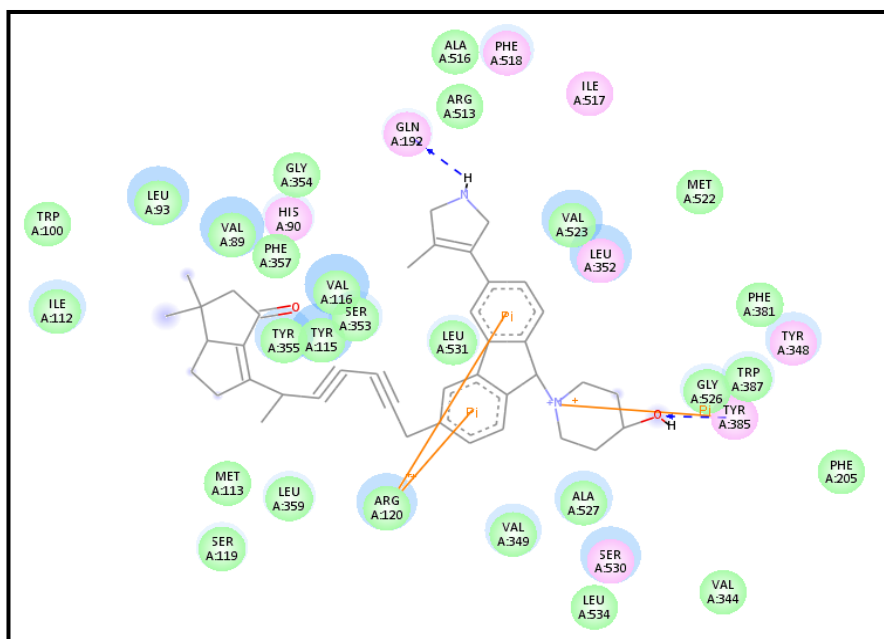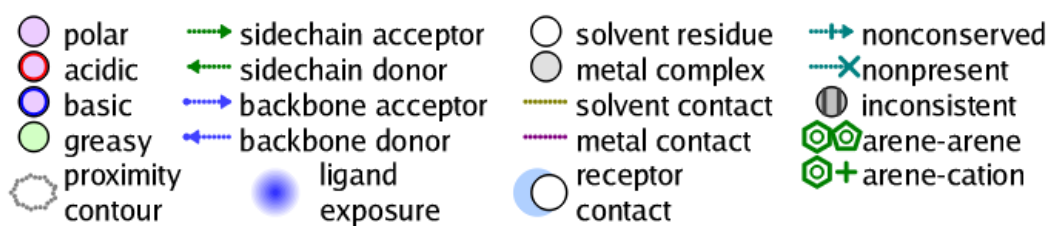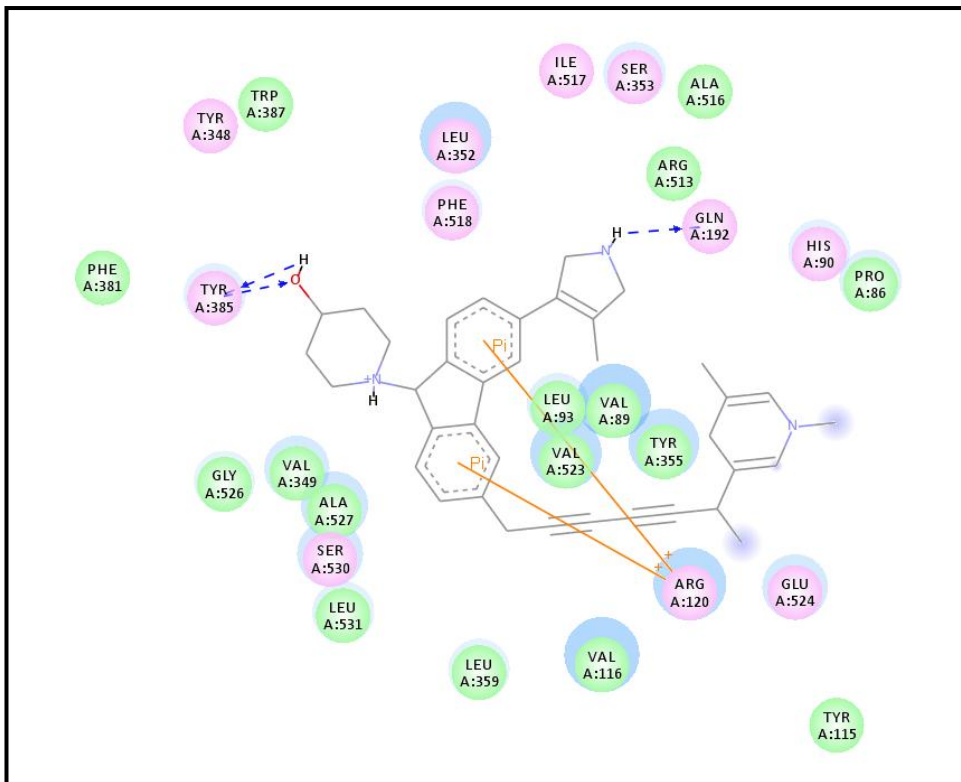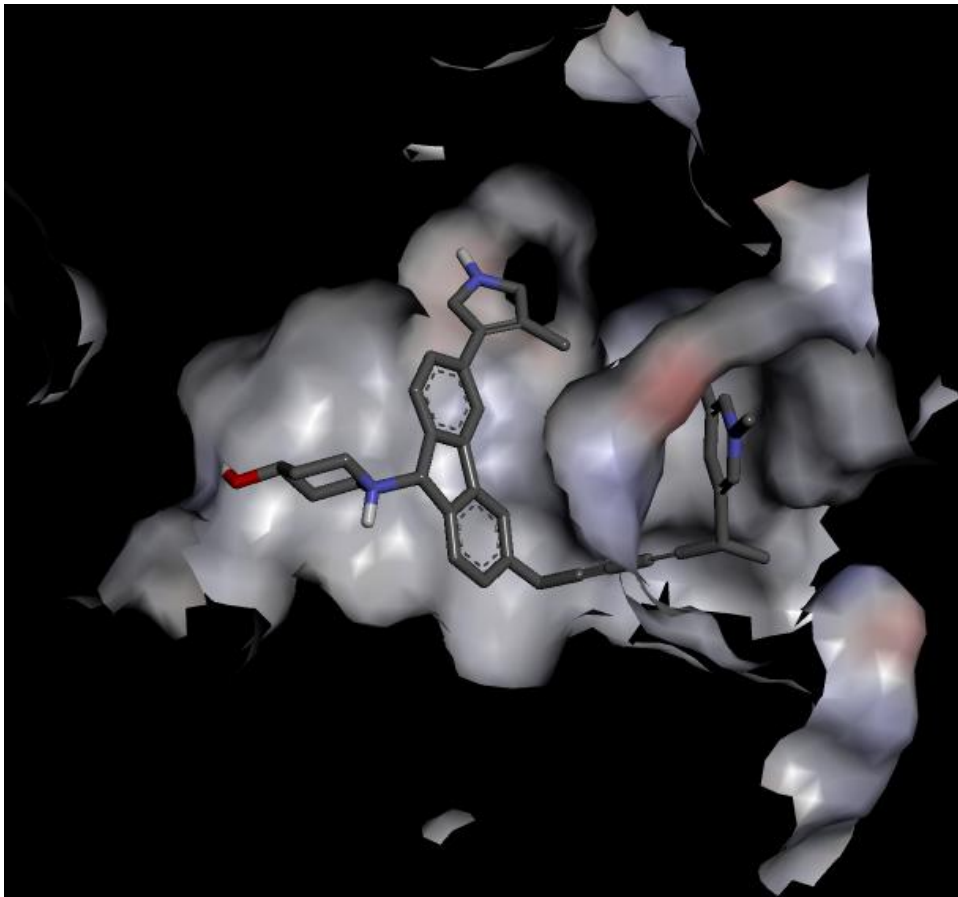

Figure 4. 16: 2-D interaction diagram of ligand TM_01 with COX-2
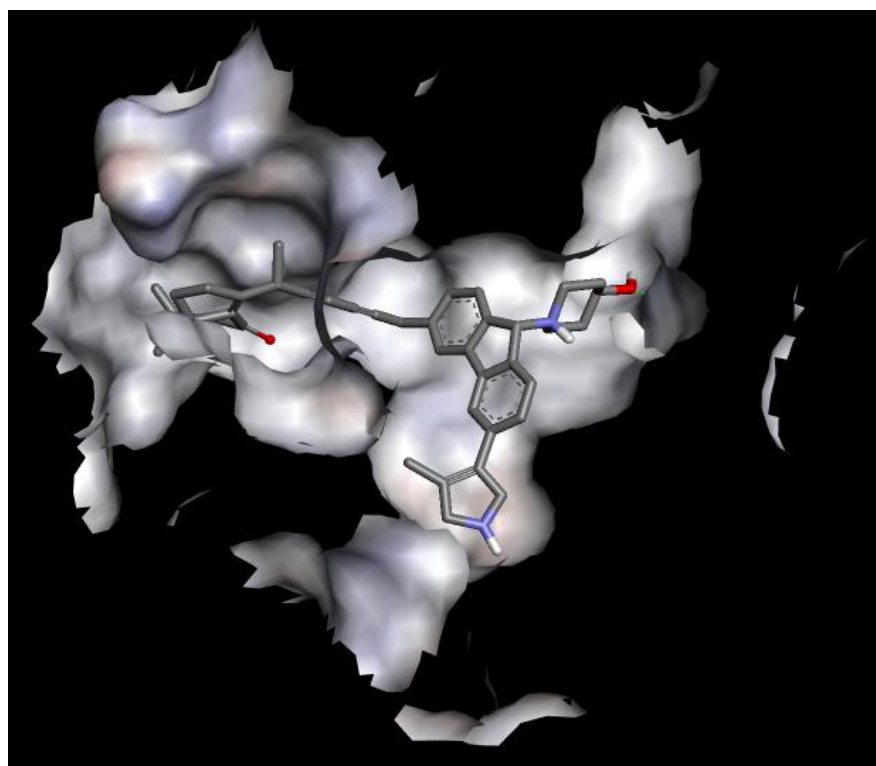
Figure 4. 17: COX-2 enzyme surface around ligand TM_01

45
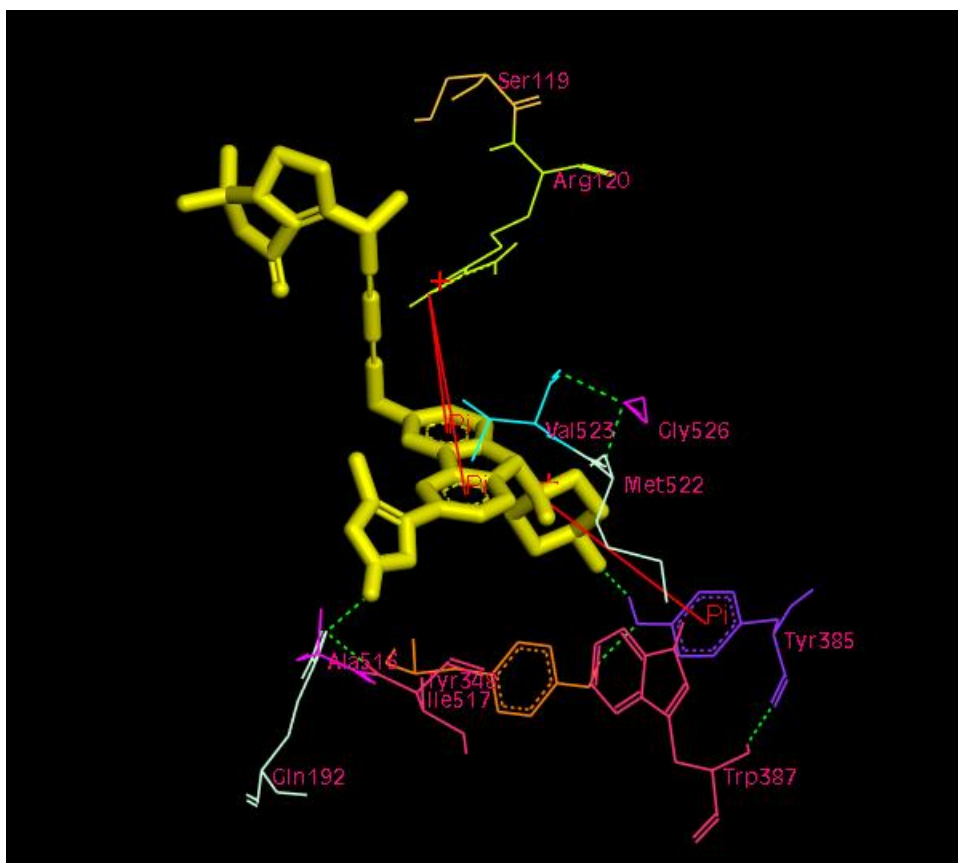
Figure 4. 18: Interacting residues of COX-2 with TM_01
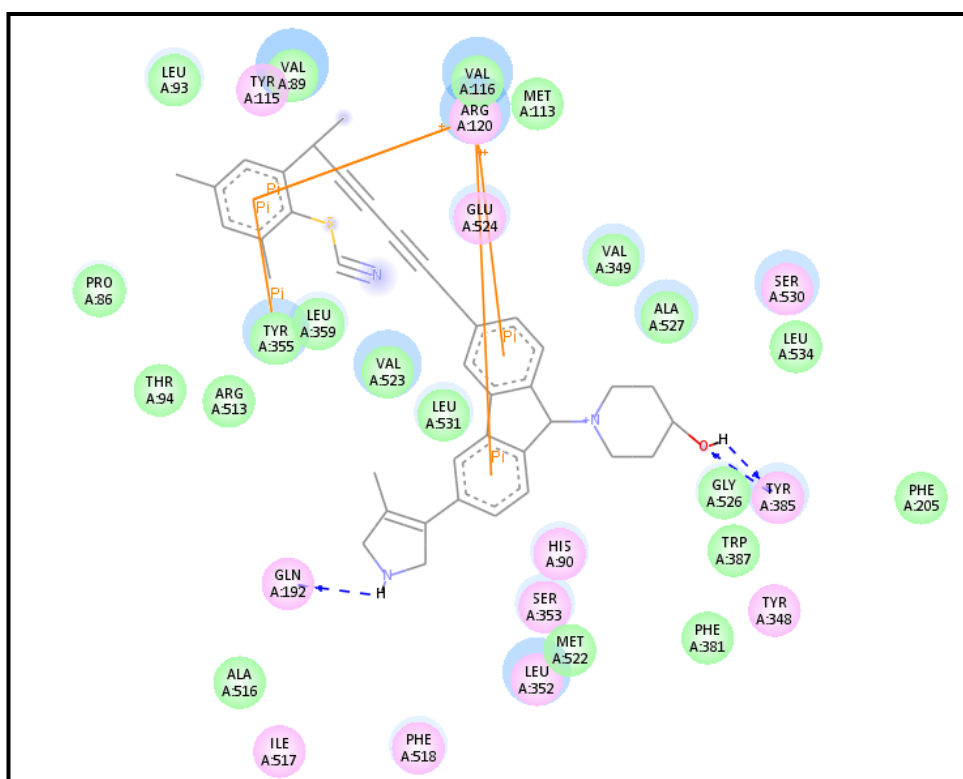
Figure 4. 19: 2-D interaction diagram of ligand TM_02 with COX-2

46
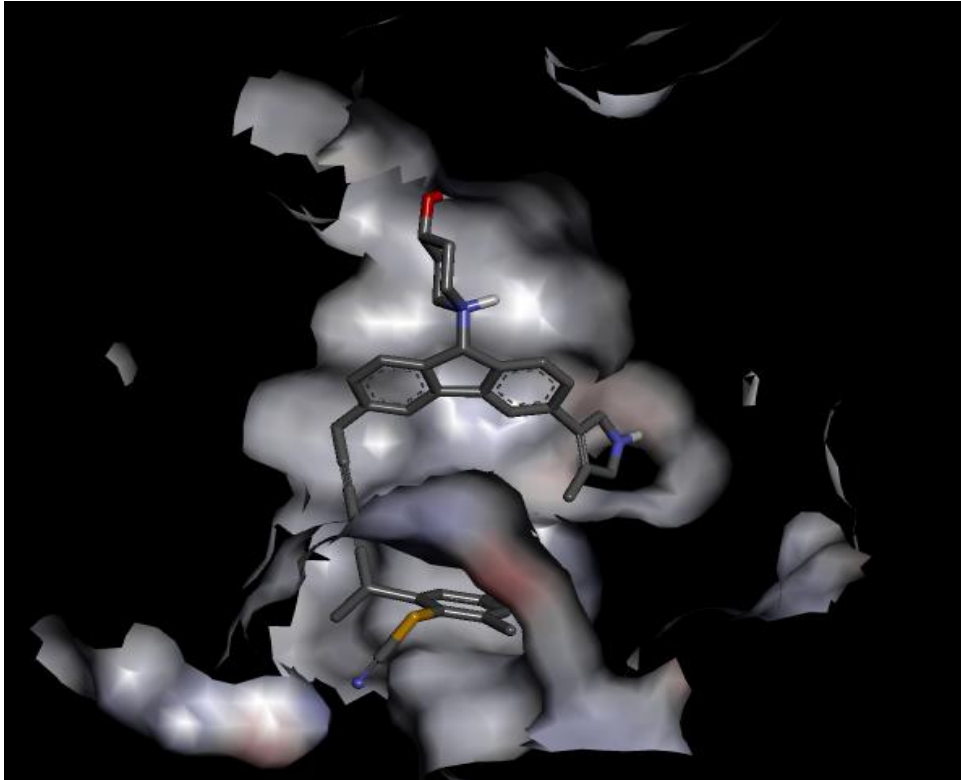
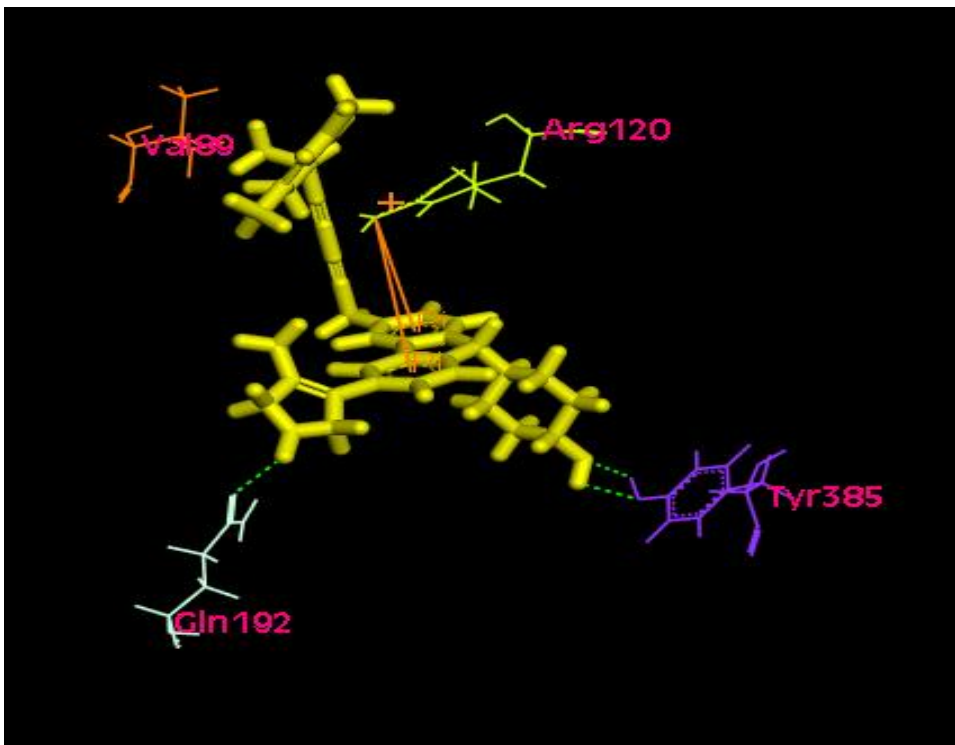**Figure 4. 20:** COX-2 enzyme surface around ligand TM_02

Figure 4. 21: 2-D interaction diagram of ligand TM_04 with COX-2

Figure 4. 22: COX-2 enzyme surface around ligand TM_04

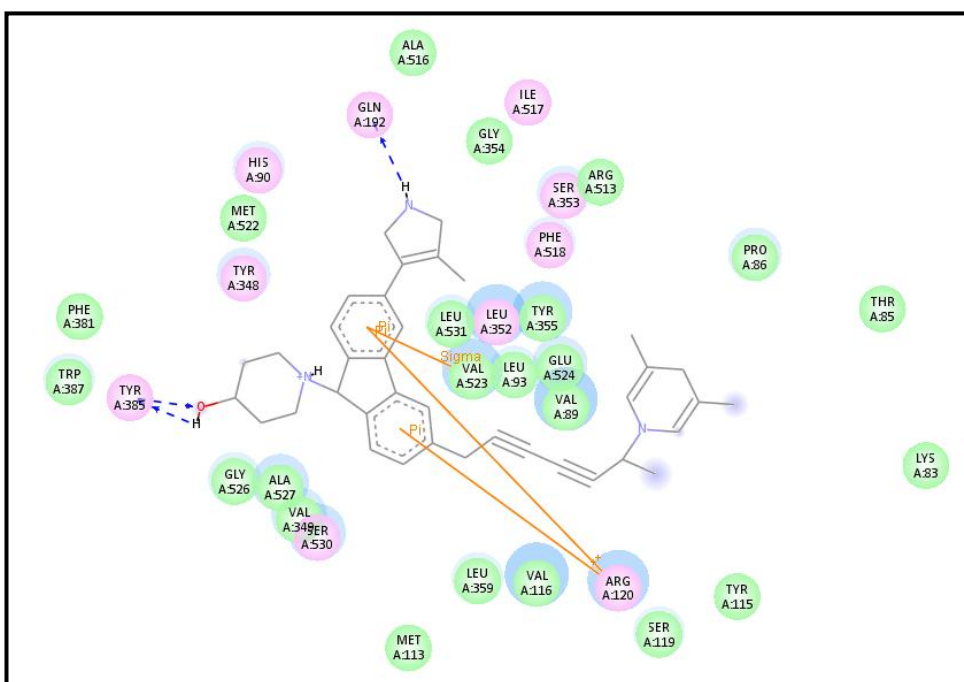
Figure 4. 23: Interacting residues of COX-2 with TM_04

48

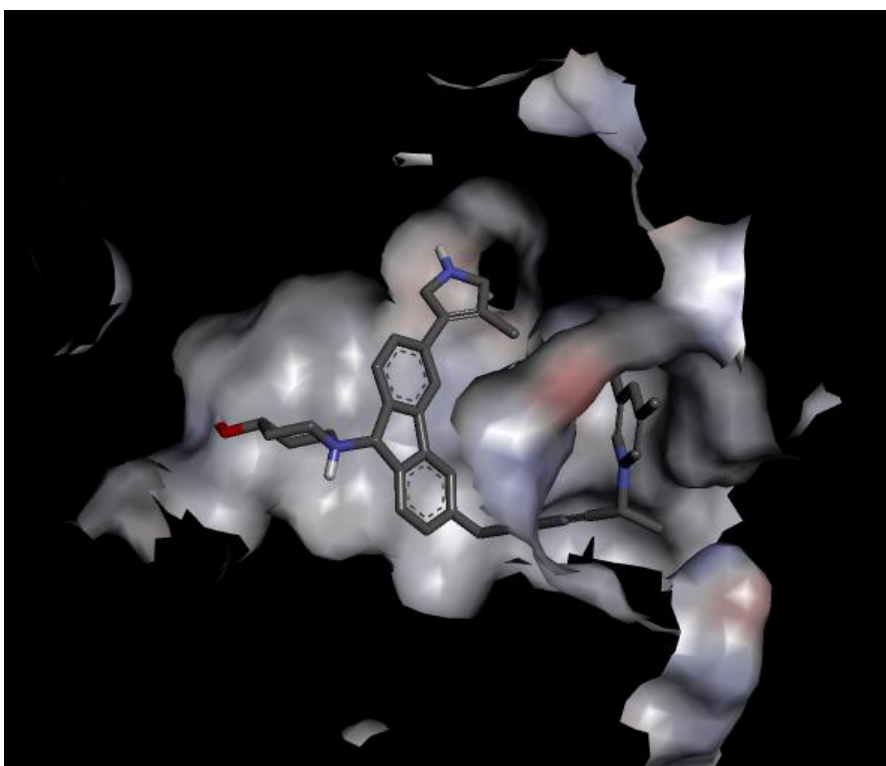**Figure 4. 24:** 2-D interaction diagram of ligand TM_07 with COX-2

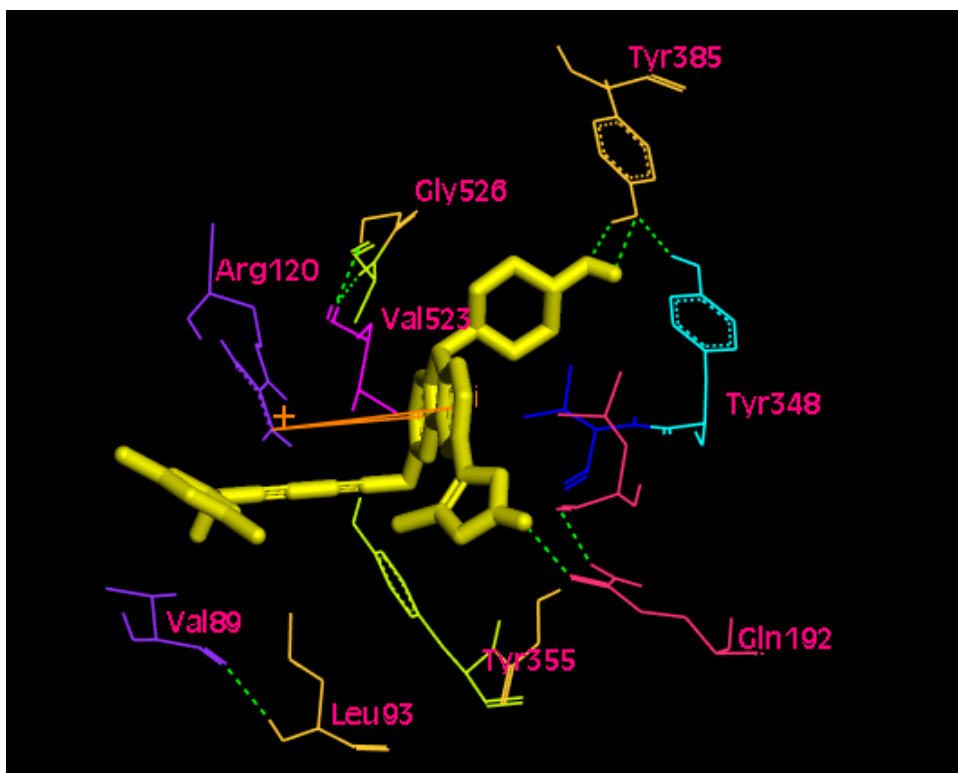**Figure 4. 25:** COX-2 enzyme surface around ligand TM_07

Figure 4. 26: Interacting residues of COX-2 with TM_07
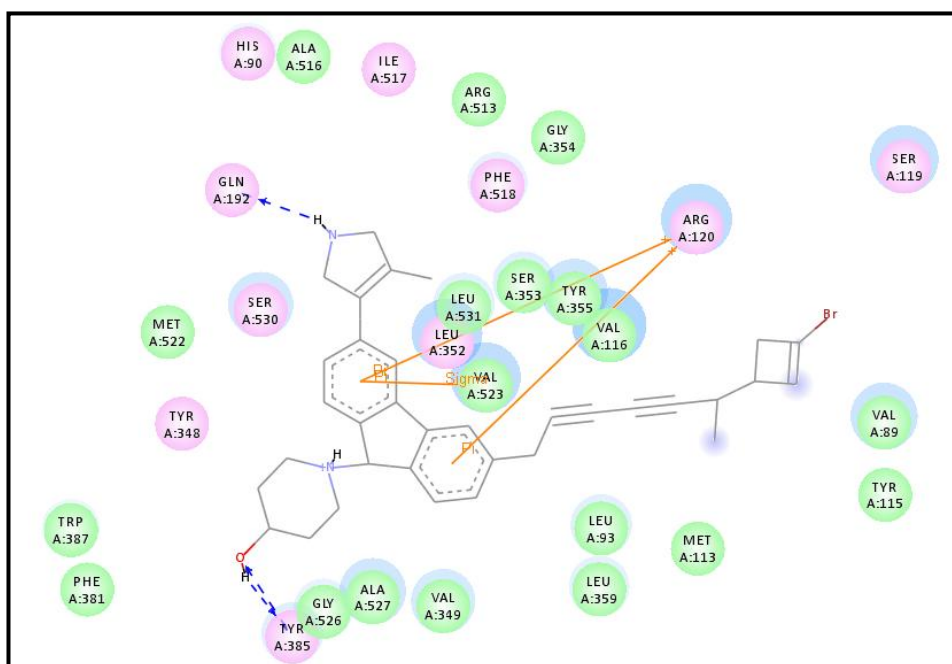

Figure 4. 27: 2-D interaction diagram of ligand TM_09 with COX-2
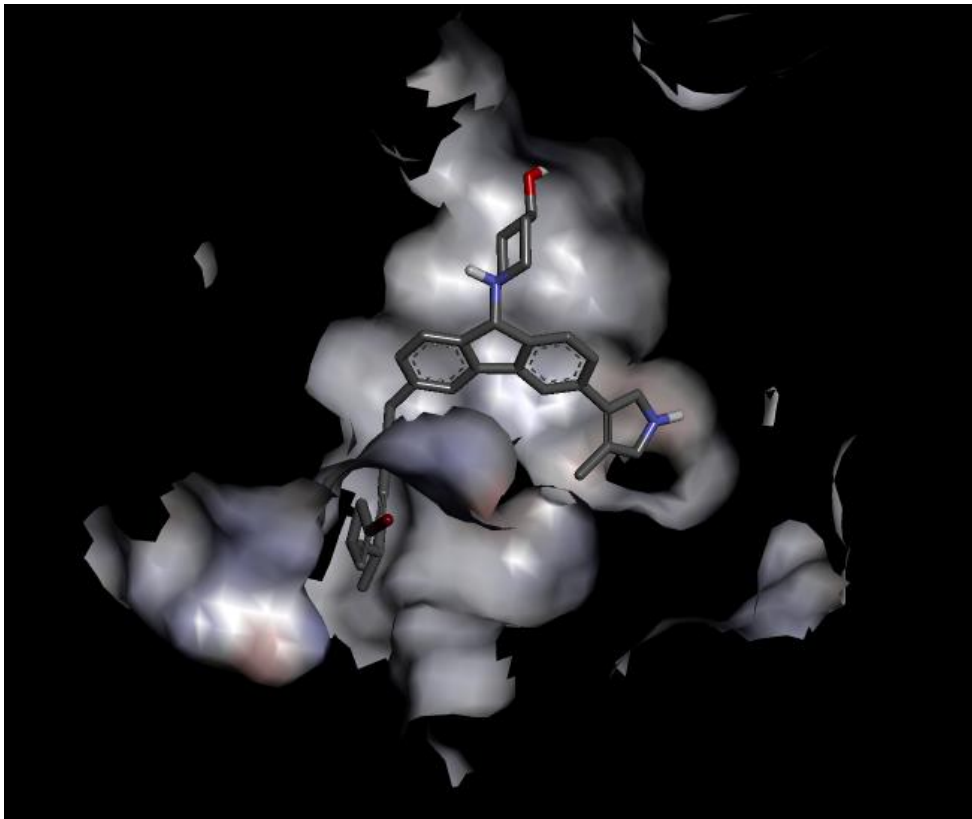
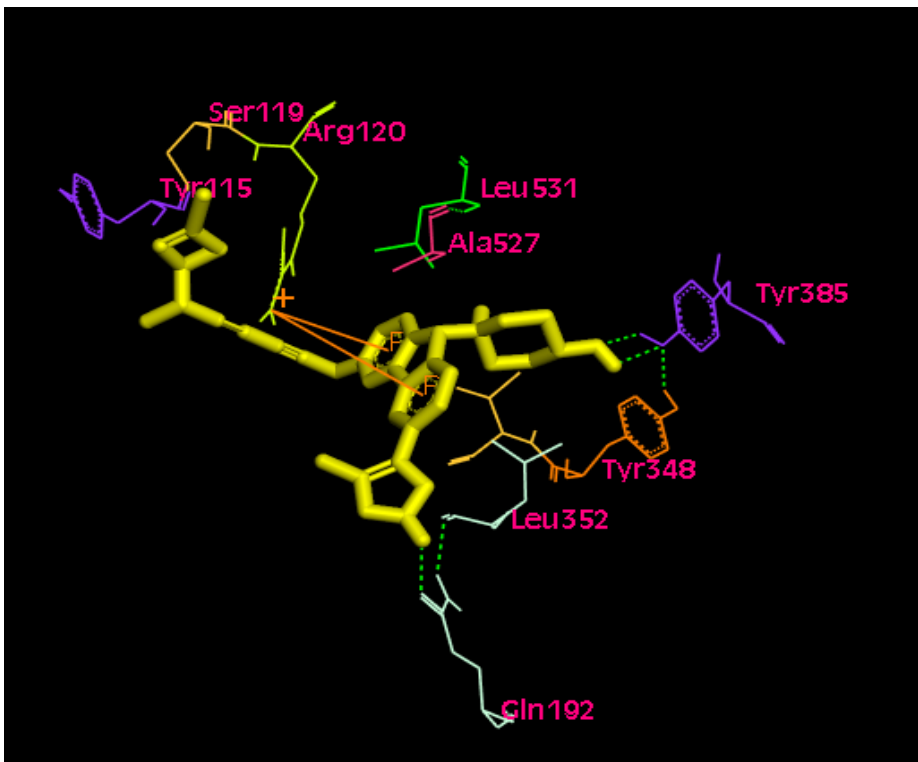**Figure 4. 28:** COX-2 enzyme surface around ligand TM_09

Figure 4. 29: Interacting residues of COX-2 with TM_09

Figure 4. 30: 2-D interaction diagram of ligand TM_12 with COX-2

Figure 4. 31: COX-2 enzyme surface around ligand TM_12

Figure 4. 32: Interacting residues of COX-2 with TM_12

Figure 4. 33: 2-D interaction diagram of ligand TM_16 with COX-2

Figure 4. 34: COX-2 enzyme surface around ligand TM_16
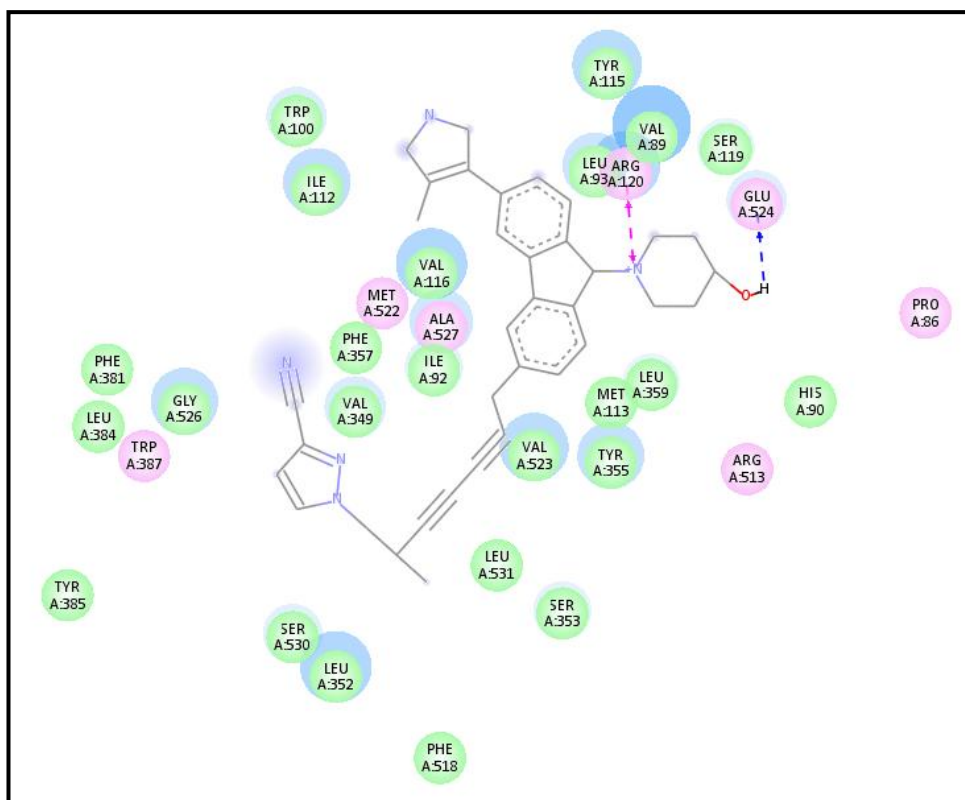

Figure 4. 35: Interacting residues of COX-2 with TM_16

Figure 4. 36: 2-D interaction diagram of ligand TM_18 with COX-2

Figure 4. 37: COX-2 enzyme surface around ligand TM_18

Figure 4. 38: 2-D interaction diagram of ligand TM_24 with COX-2

Figure 4. 39: COX-2 enzyme surface around ligand TM_24

Figure 4. 40: 2-D interaction diagram of ligand TM_27 with COX-2
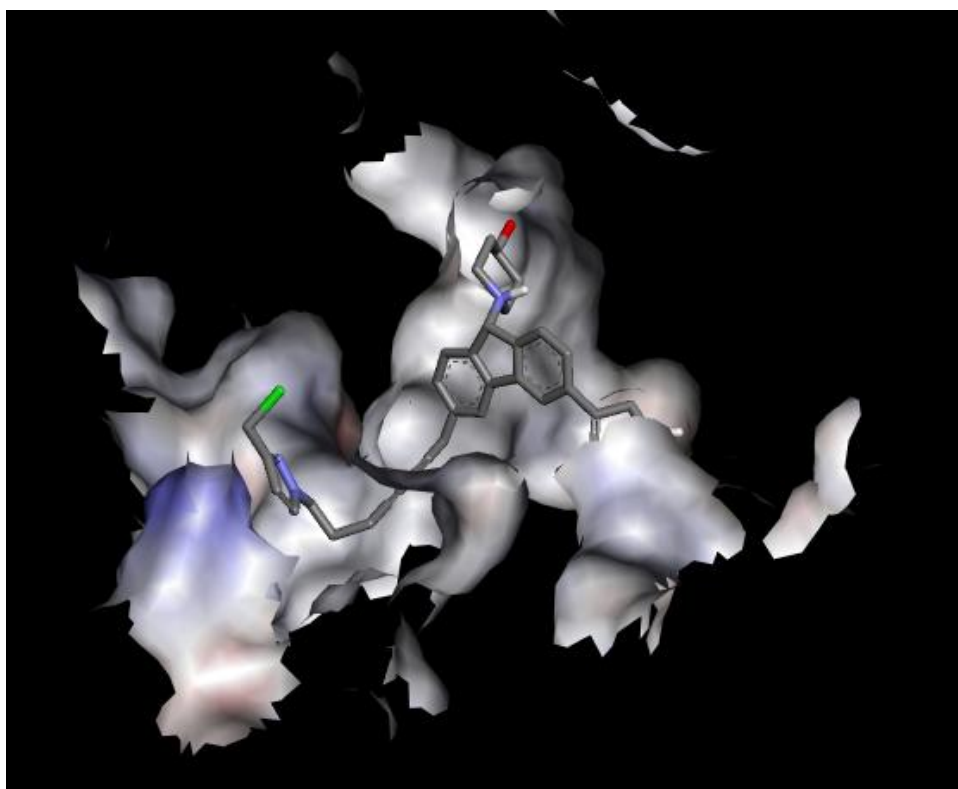
Figure 4. 41: COX-2 enzyme surface around ligand TM_27
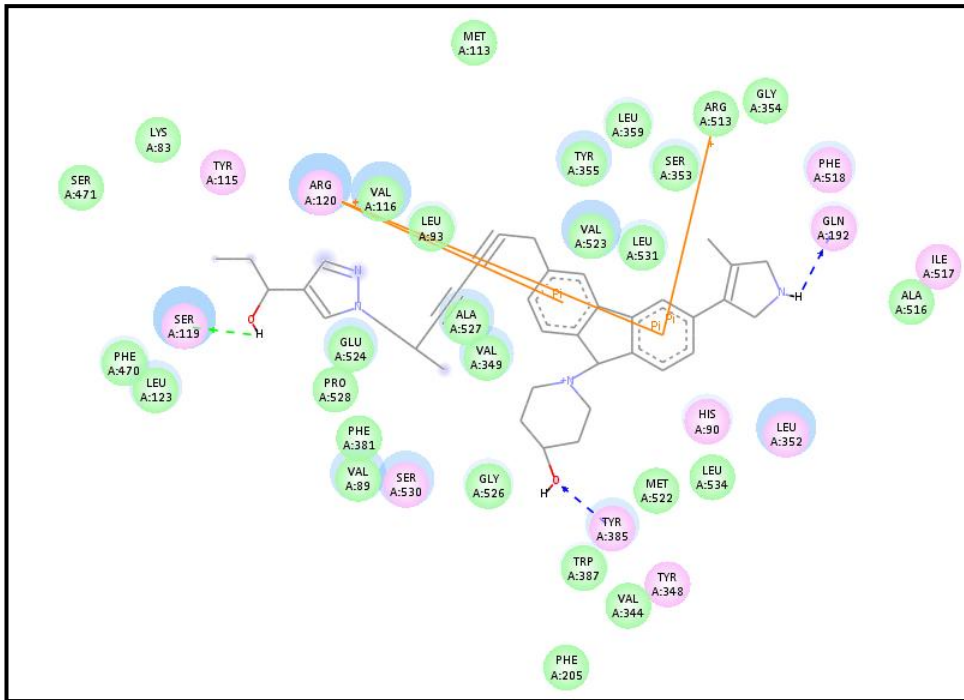
Figure 4. 42: 2-D interaction diagram of ligand TM_28 with COX-2

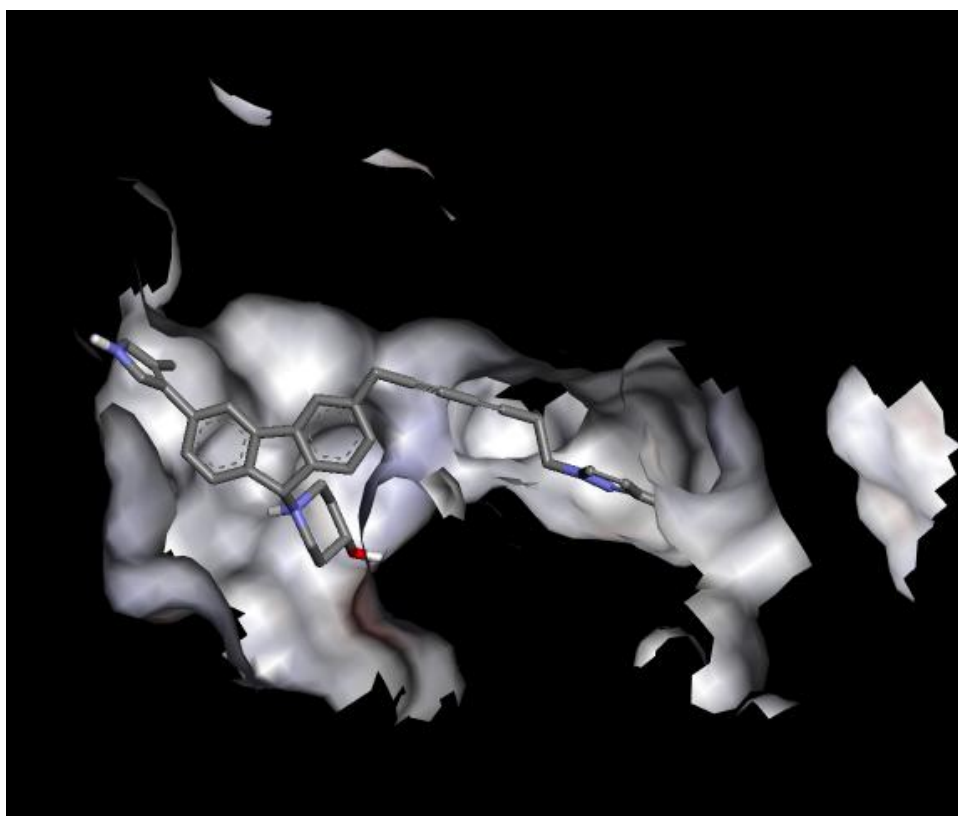**Figure 4. 43:** COX-2 enzyme surface around ligand TM_28

58
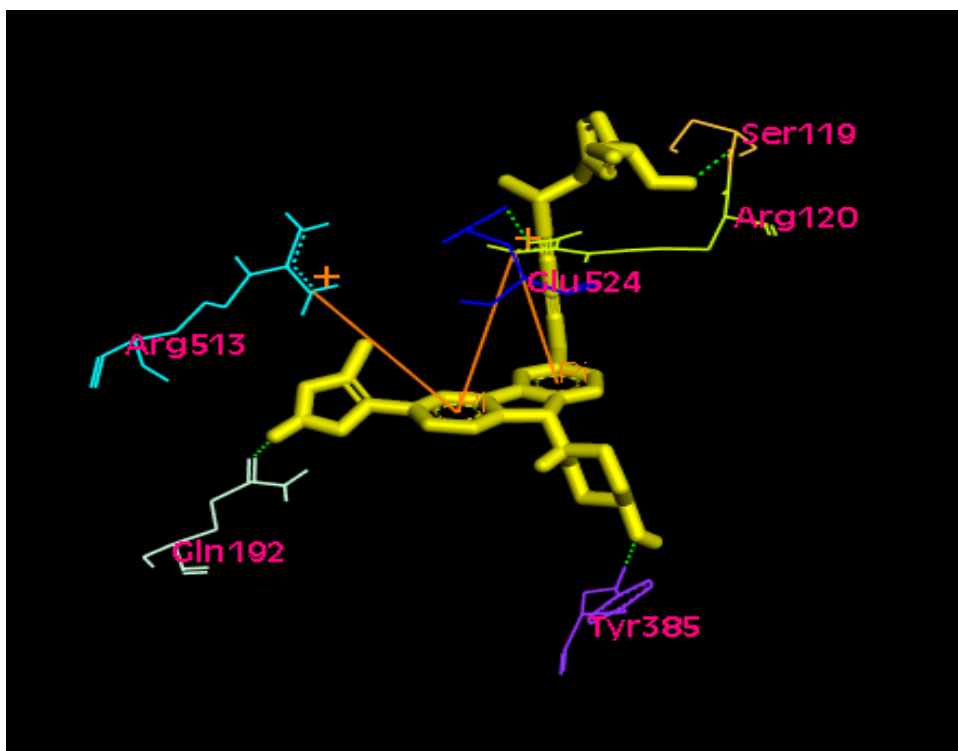
Figure 4. 44: Interacting residues of COX-2 with TM_28
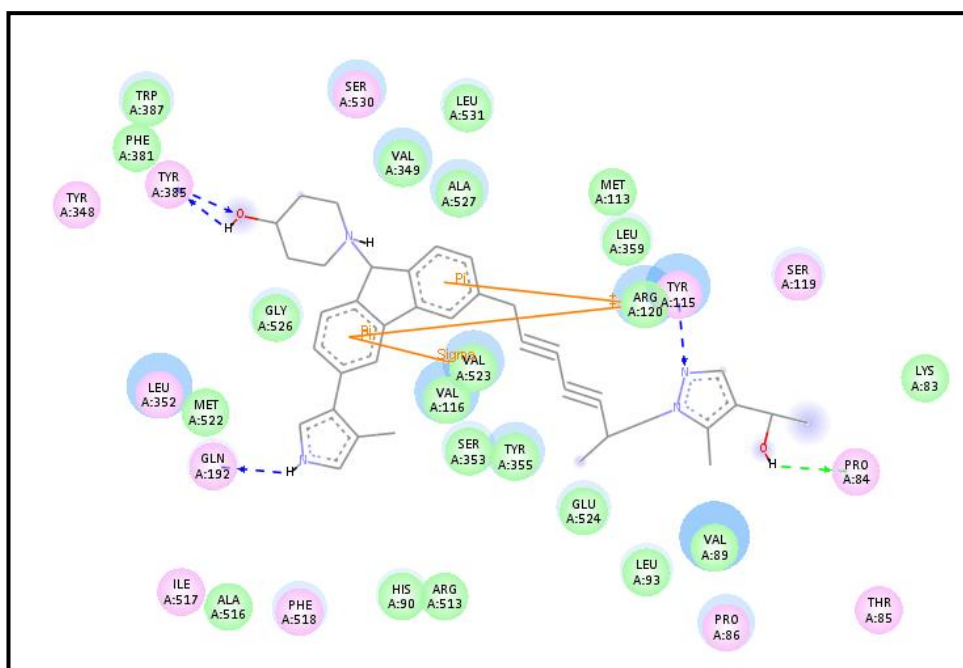
Figure 4. 45: 2-D interaction diagram of ligand TM_31 with COX-2
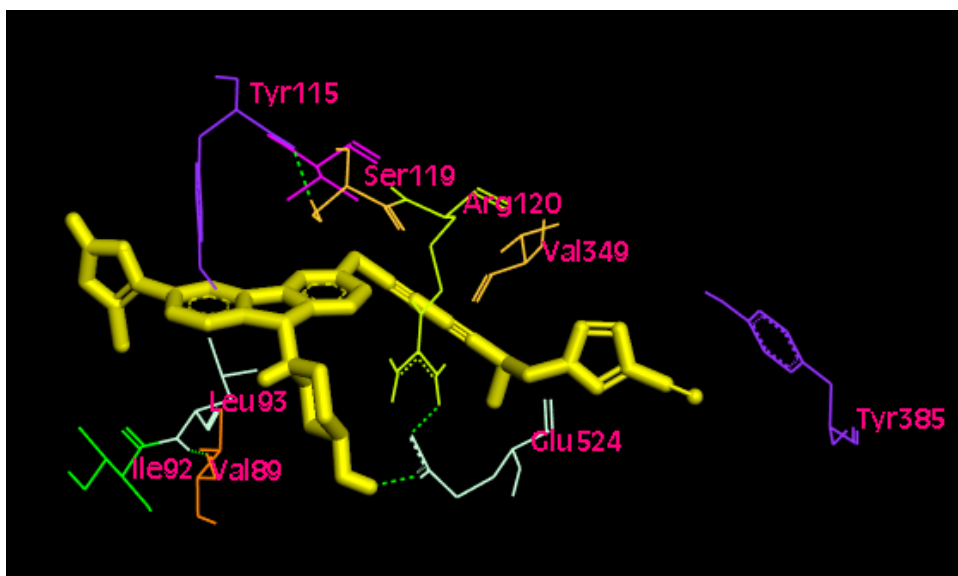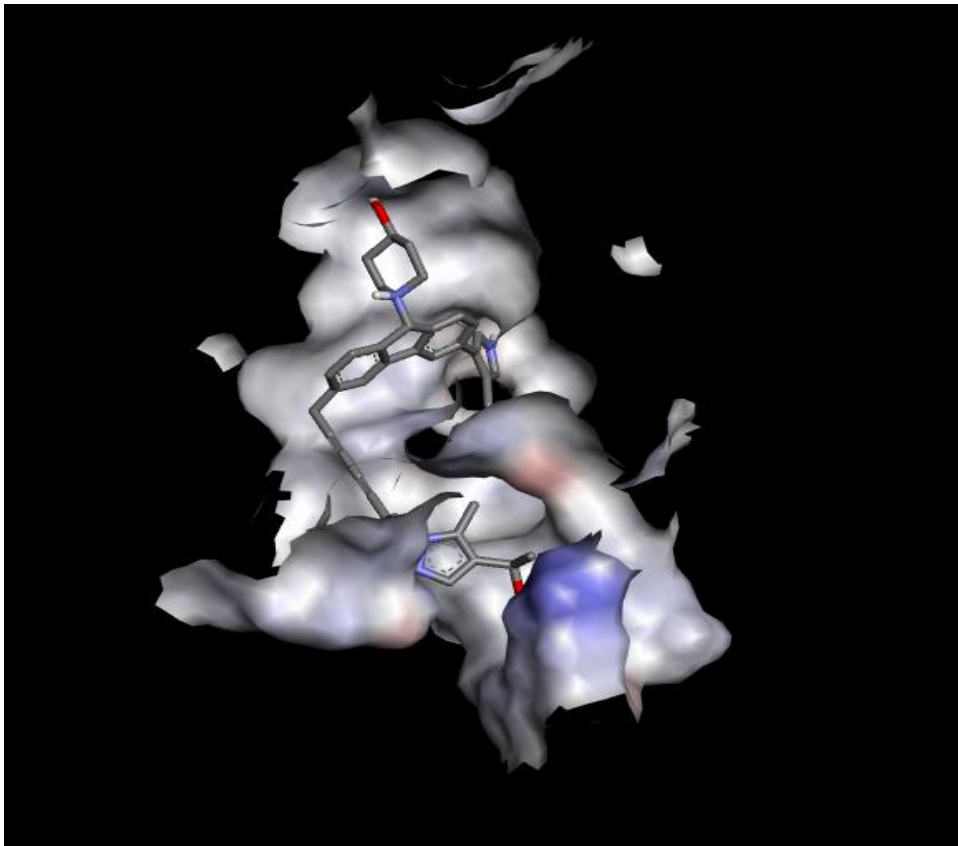
Figure 4. 46: COX-2 enzyme surface around ligand TM_31
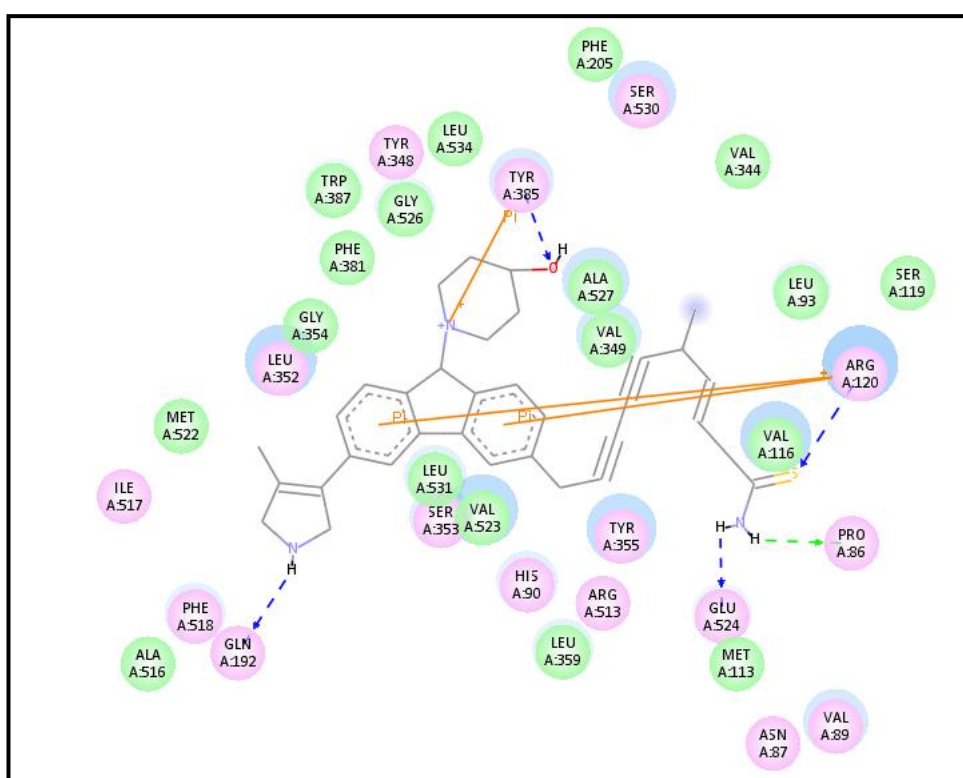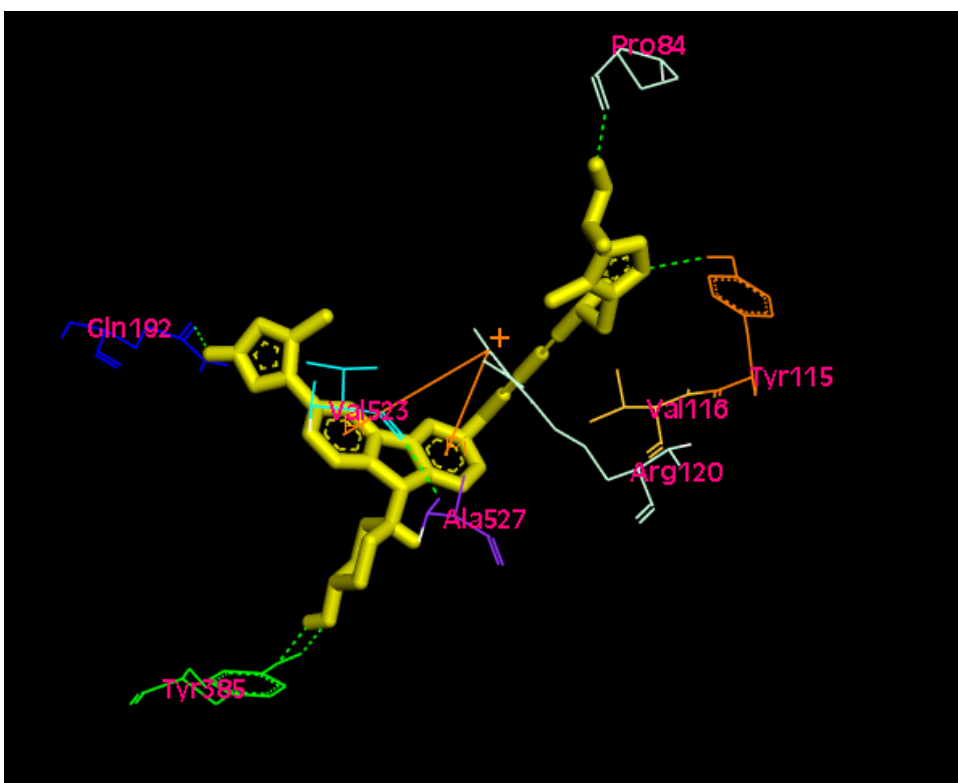

Figure 4. 47: Interacting residues of COX-2 with TM_31
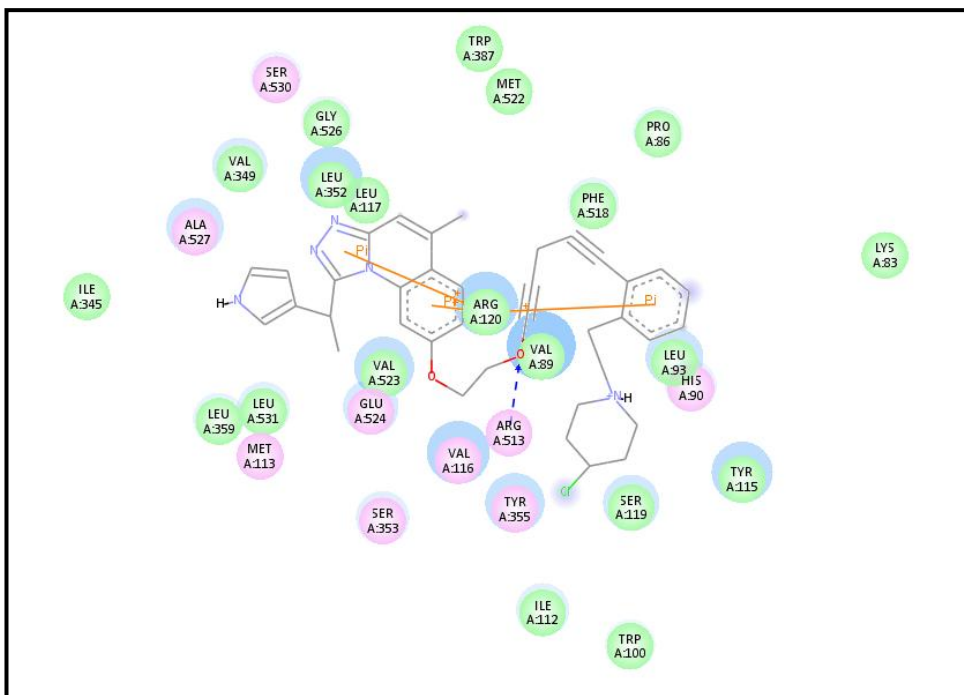
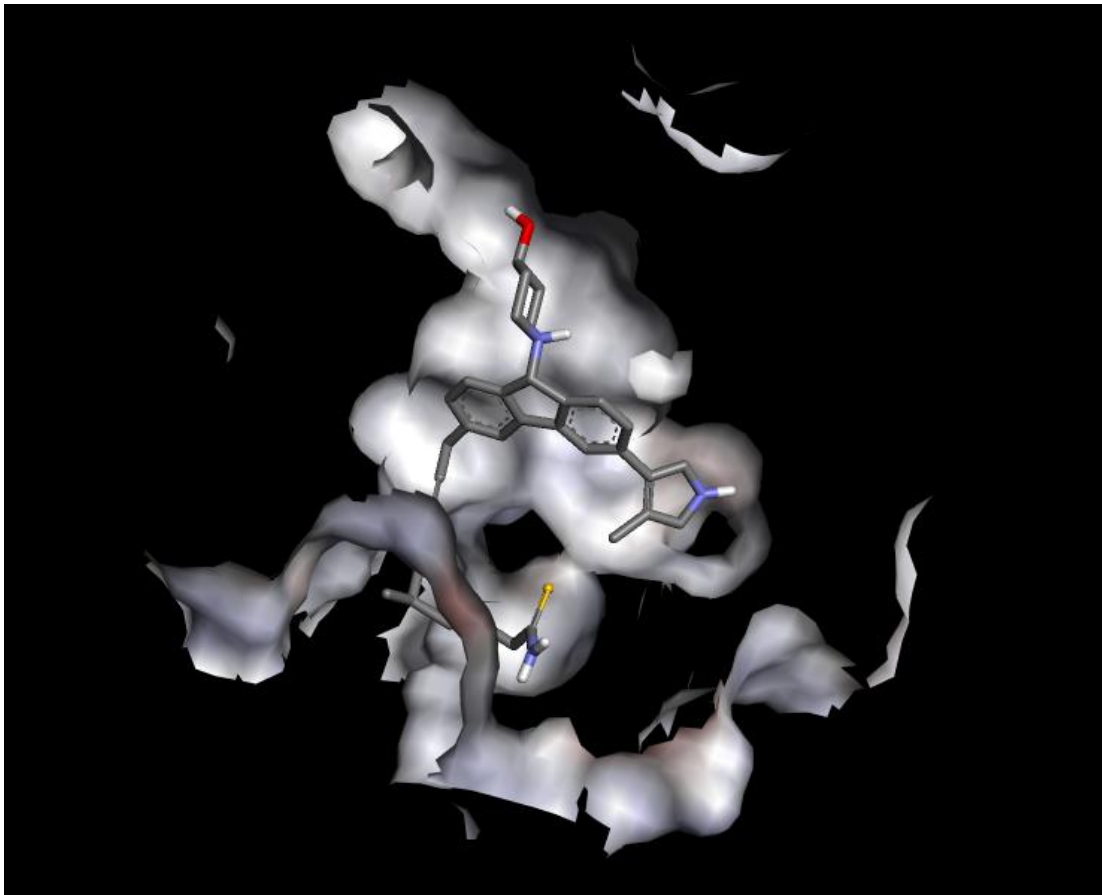**Figure 4. 48:** 2-D interaction diagram of ligand TM_34 with COX-2

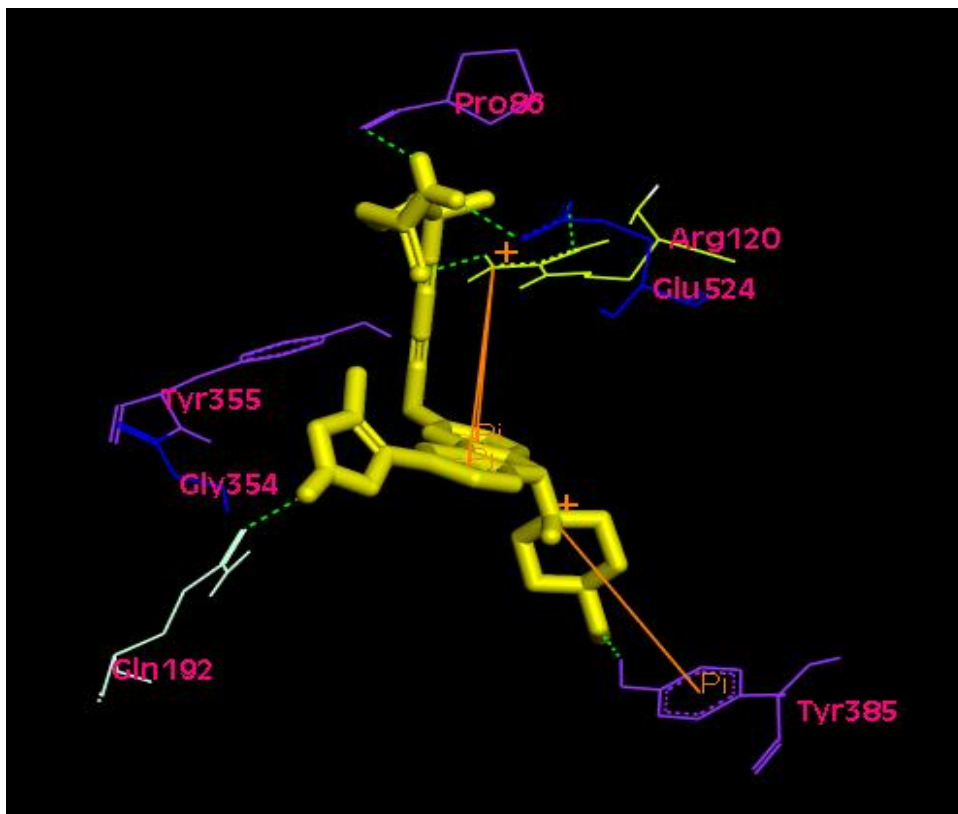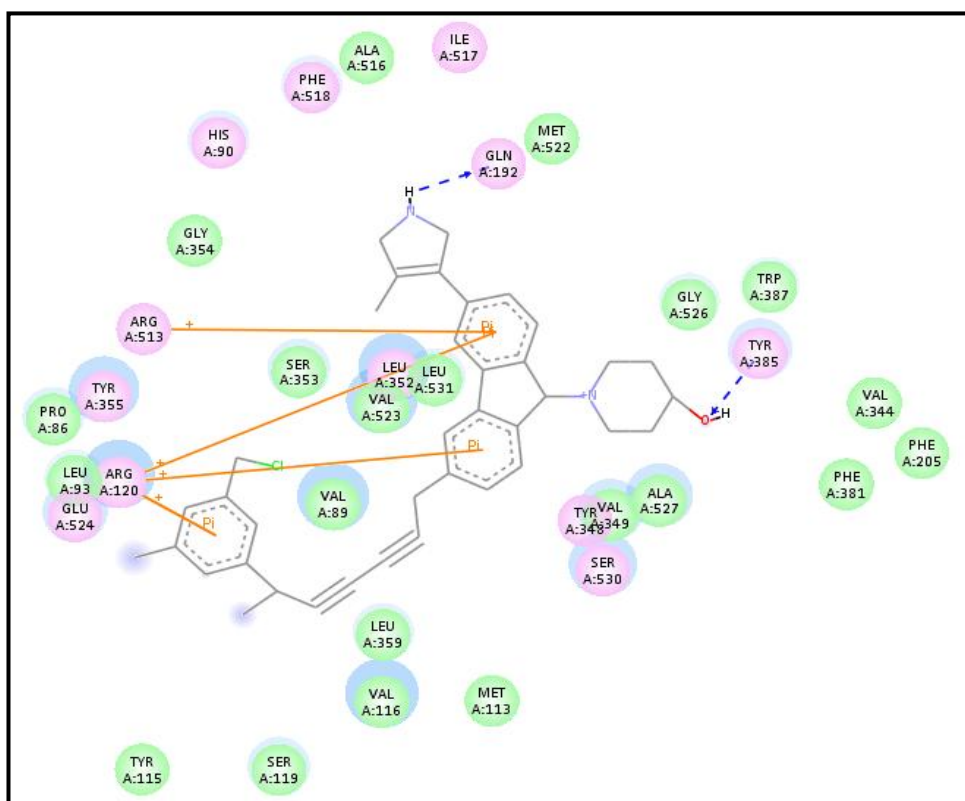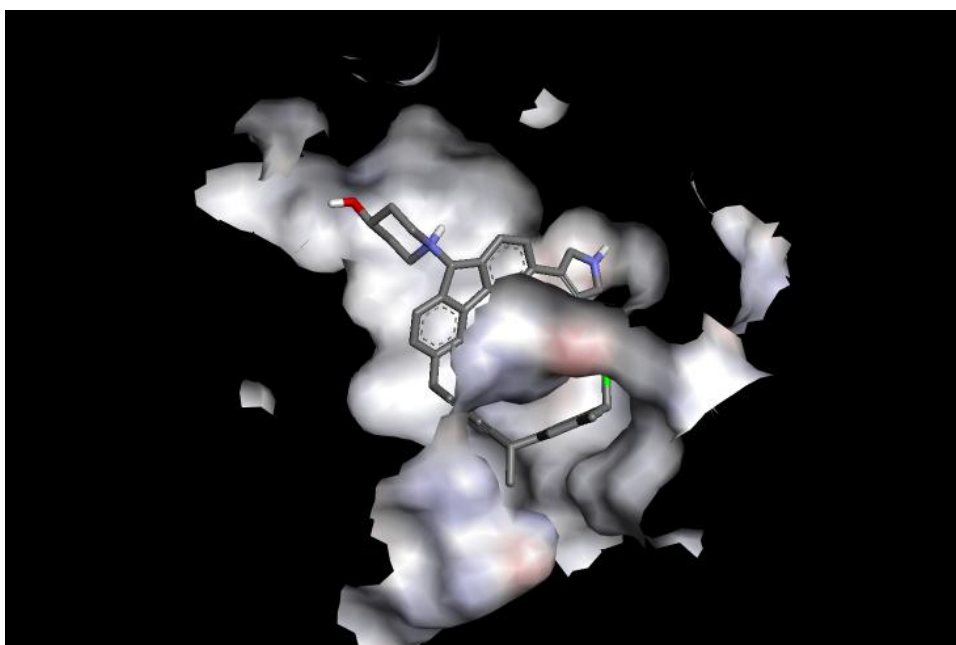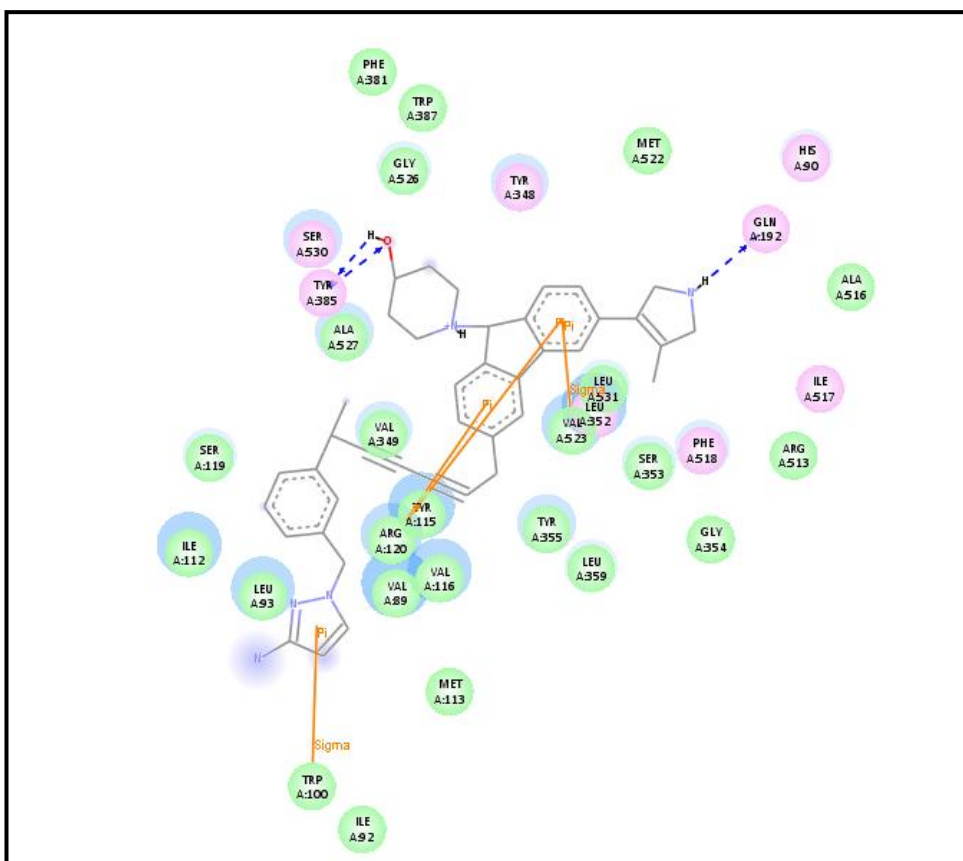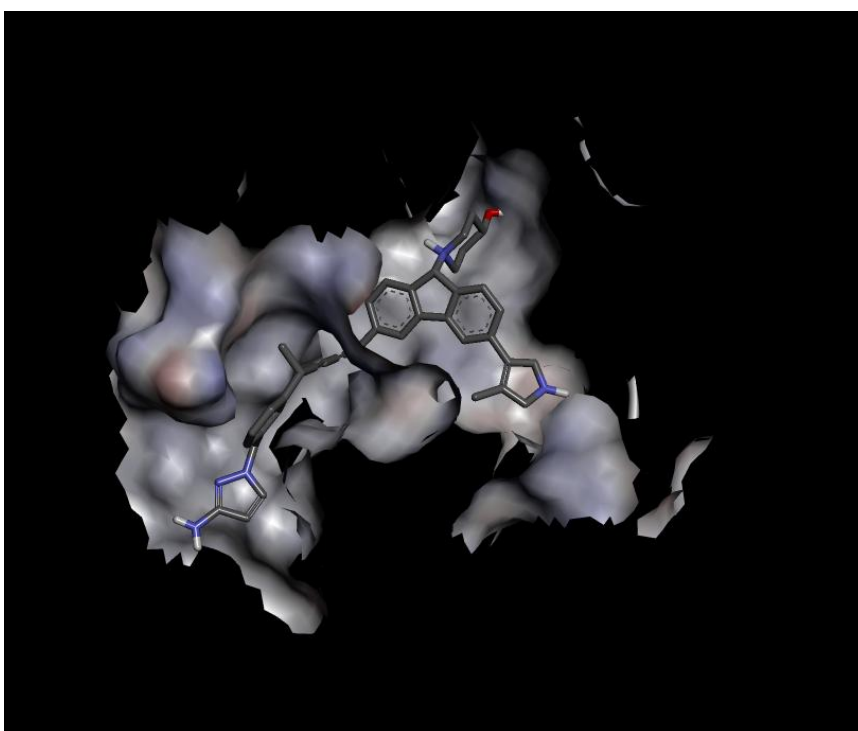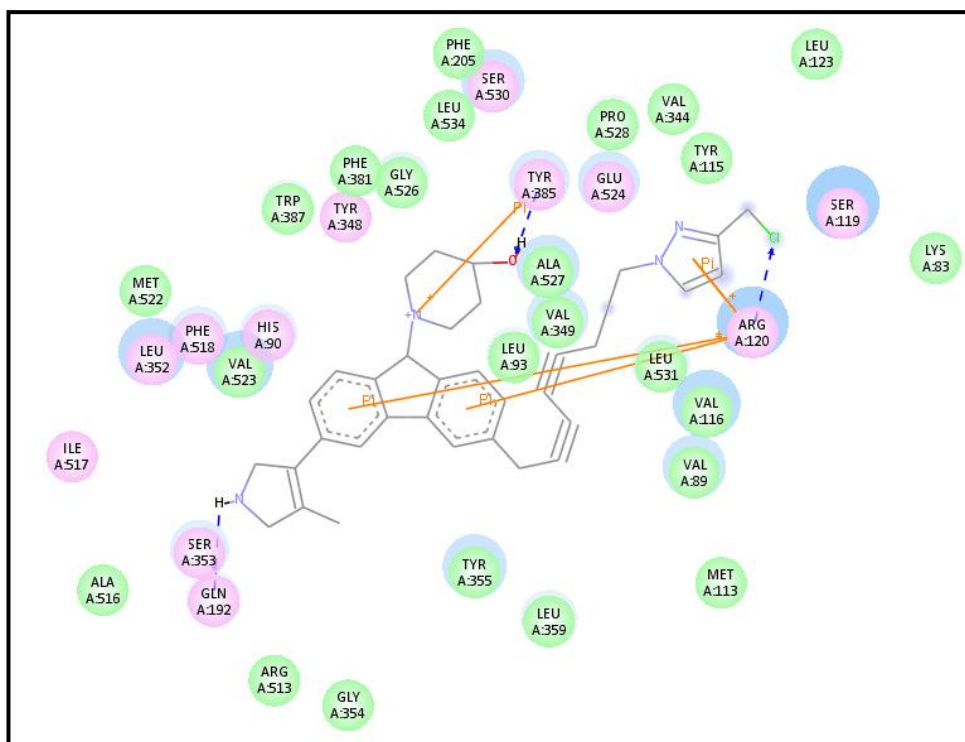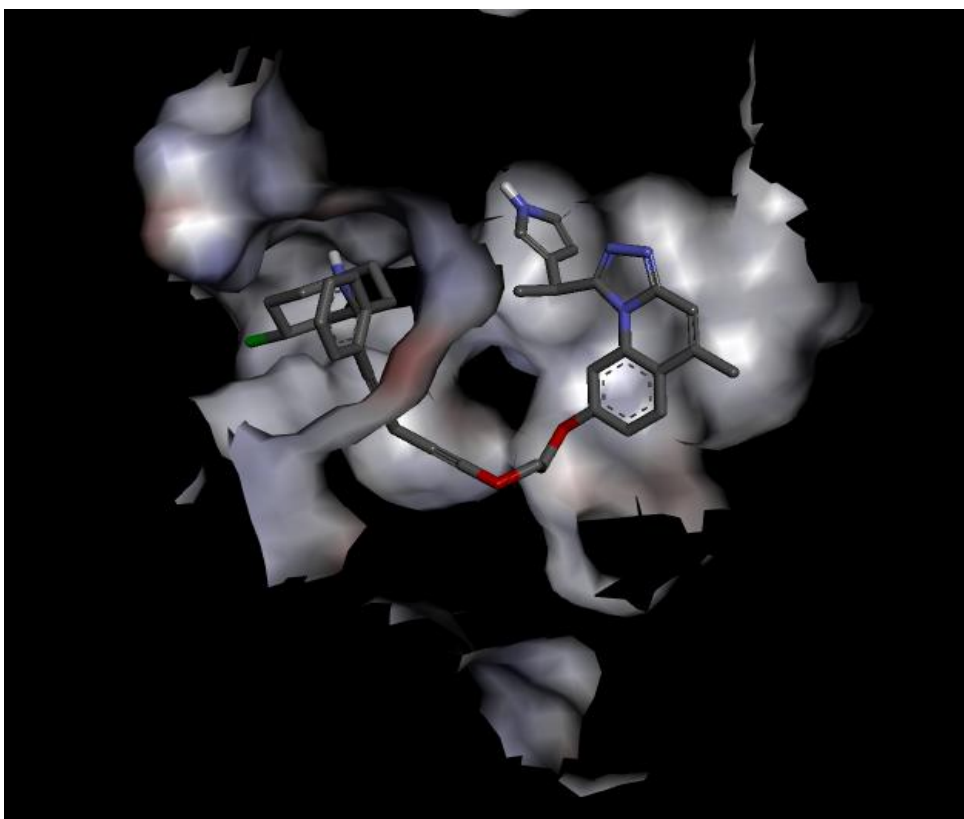**Figure 4. 49:** COX-2 enzyme surface around ligand TM_34

61
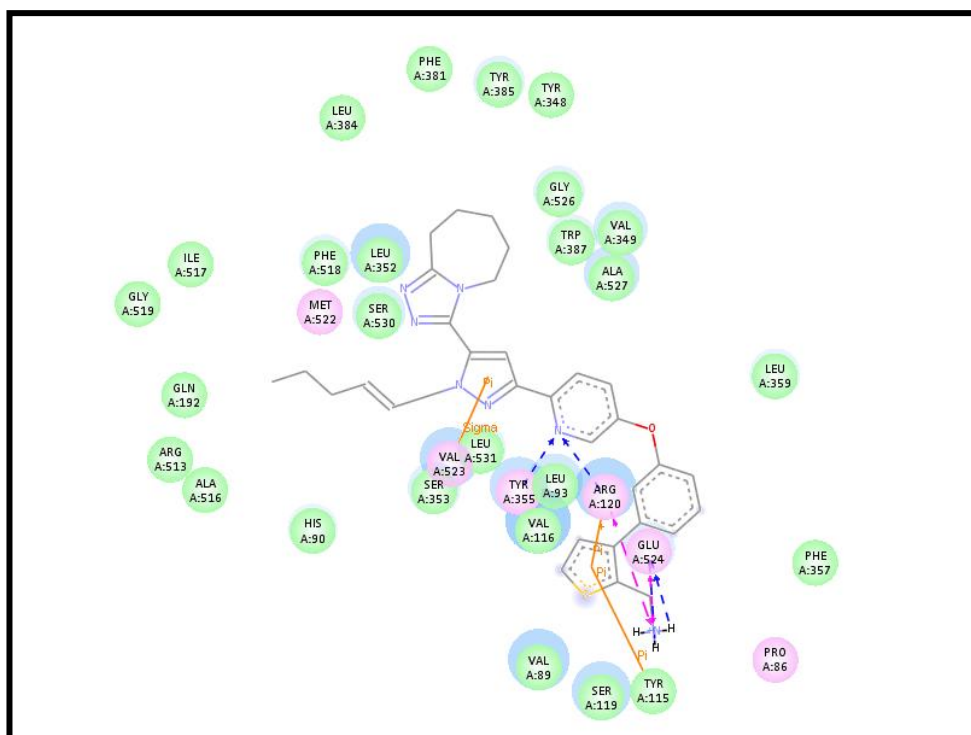
Figure 4. 50: 2-D interaction diagram of ligand TM_v_20 with COX-2
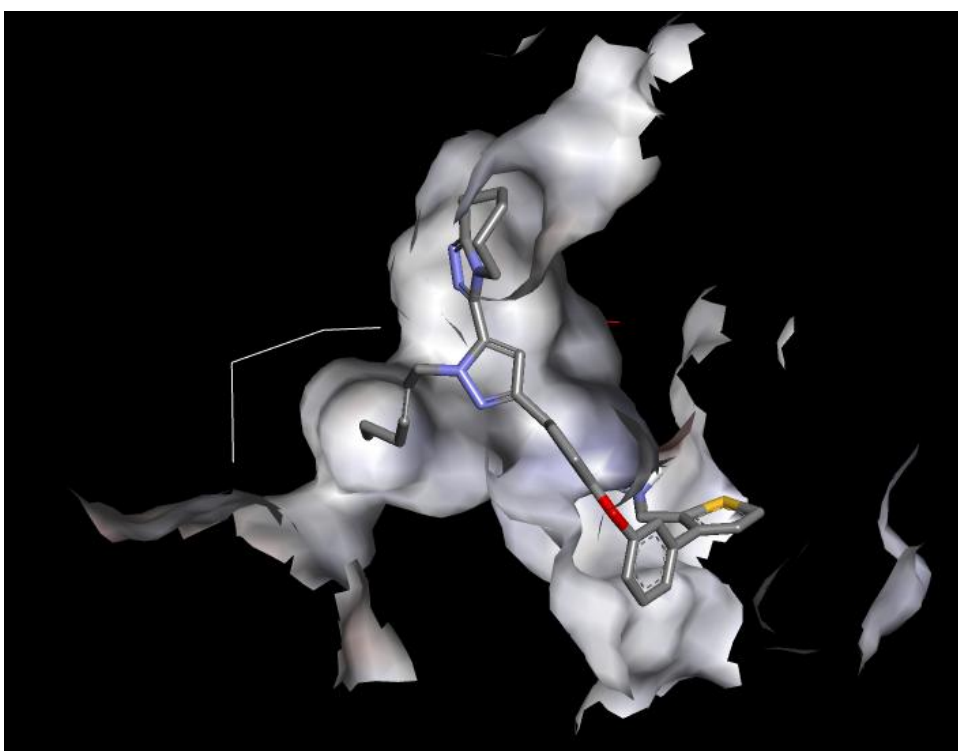
Figure 4. 51: COX-2 enzyme surface around ligand TM_v_20

4.3 ADMET results
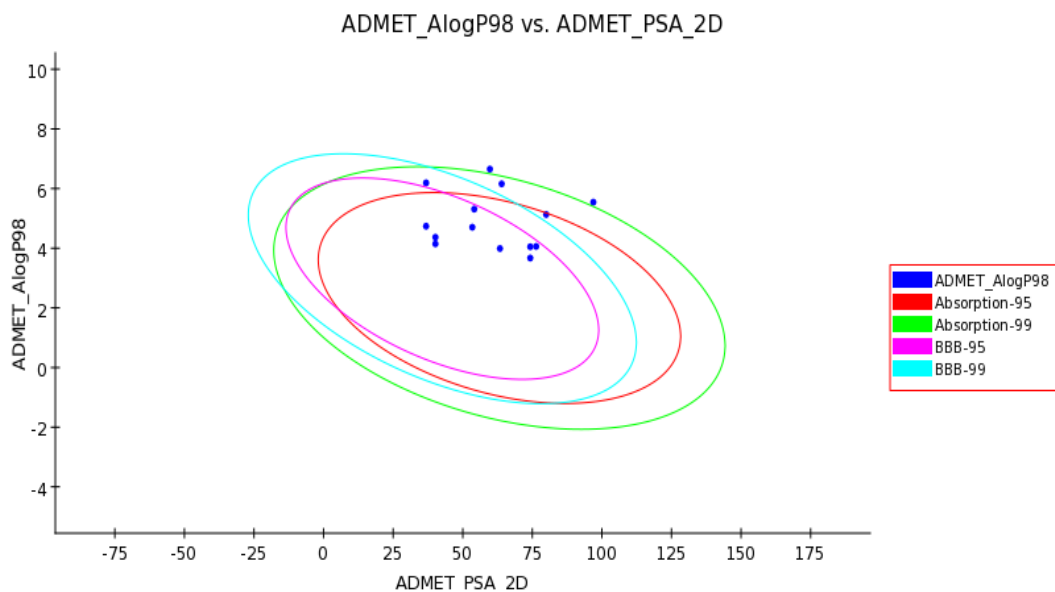
Figure 4. 52: ADMET results

ADMET test filters poor candidates with undesirable chemical groups according to published SMARTS, Lipinski and Veber rules. Currently available ADMET models expect human intestinal absorption (HIA) after oral administration. ADMET aqueous solubility: predicts the solubility of each compound in water at 25°C. ADMET blood brain barrier: predicts the ratio of concentrations of compound on both sides of the blood brain membrane after oral administration. ADMET plasma protein binding: predicts whether or not a compound is prone to be highly bound to carrier proteins in the blood. ADMET CYP2D6 binding: predicts cytochrome P450 2D6 enzyme inhibition. ADMET hepatotoxicity: predicts dose-dependent human, hepatoxicity of compounds. Atom based Log P98 (A LogP 98), ADMET 2D polar surface area (ADMET 2D PSA), Blood Brain Barrier penetration (BBB-95 and BBB-99).

ADMET experiment was calculated for ADMET_AlogP98, Absoption-99, Absorbtion-95, BBB-95 and BBB-99. As shown in Figure 4.52, 3 ligands are

rounded by a green circle (ABP 99), 2 are encircled by BBB-95 and BBB-99. Remaining 8 are all in the circles, which is the safe area. Namely these compounds are; TM_01, TM_04, TM_07, TM_09, TM_12, TM_16, TM_27, TM_28, and TM_31.

This shows the usability of ligands against COX-2 enzyme as drugs. This means that 8 of the selected results are perfect drug candidates according to ADMET simulation. Detailed explanation for the names that either passed or failed ADMET test can be found in Table 4.8.

Original names of ligands were expressed below. Red highlight means ligands that could not pass ADMET and green highlight means ligands that passed ADMET.

Table 4. 8: Result of ADMET

COX-1 based ligands	
TM_v_20	TM_2013_04_07_151011_894-7-35
COX-2 based ligands	
TM_01	TM_2013_05_17_230538_994-10--1.pdb
TM_02	TM_2013_05_17_230538_994-10--33.pdb
TM_04	TM_2013_05_17_230538_994-10--22.pdb
TM_07	TM_2013_05_17_230538_994-10--23.pdb
TM_09	TM_2013_05_17_230538_994-10--18.pdb
TM_12	TM_2013_05_17_230538_994-10--41.pdb
TM_16	TM_2013_05_17_230538_994-10--43.pdb
TM_18	TM_2013_05_17_230538_994-10--19.pdb
TM_24	TM_2013_05_17_230538_994-10--44.pdb
TM_27	TM_2013_05_17_230538_994-10--36.pdb
TM_28	TM_2013_05_17_230538_994-10--25.pdb
TM_31	TM_2013_05_17_230538_994-10--5.pdb
TM_34	**TM_2013_05_17_231259_735-1---4.pdb**

5. CONCLUSION

As potential drug candidates, 14 novel molecules were found to be COX-2 selective inhibitors within the scope of this work.

Celecoxib is one member of the coxib family drugs and it is a COX-2 selective inhibitor. Celecoxib, which is currently available in the market however has side effects due to slight inhibition of COX-1. It is safe to use in human therefore, it is in the market now. For this reason, the inhibition capacity and selectivity of our developed compounds were compared with the inhibition value of celecoxib and also SC-558 which is a coxib family candidate under clinical trial currently.

The compounds TM_01, TM_12 and TM_02 showed much better inhibition than that of celecoxib and our other candidate ligands. Compound TM_01 showed 3.53 fold of COX-2/COX-1 inhibition whereas same inhibition value of celecoxib is 1.23 and SC-58 is 1.27 according to GOLD program total score value. On the other hand, According to Autodock 4 program free energy folds; TM_12 showed 66.71 fold of COX-2/COX-1 inhibition whereas same free energy fold value of celecoxib is 1.25 and SC-58 is 1.24. According to GOLD program ChemPLP score value folds; TM_02 (ChemPLP score: 109,17) showed the inhibition score fold of 7.93 COX-2/COX-1. ChemPLP score values for celecoxib and SC-558 are subsequently; 58.01 and 58.19.

As a result, all the compounds that are being developed *in silico* method in our study show much better selectivity to COX-2 in comparison to celecoxib and SC-558. Due

to selection of active site as Arg 120, this amino acid is involvement is represented nearly all 2-D interaction maps and also in some highly selective candidates, Ile 523 is also involved and this residue is only present in COX-2.

Since COX-2 (1148.88 Å) has larger cavity volume constructed with 3 different amino acid than COX-1 (710.875 Å). COX-2 active site is approximately 61% larger than COX-1 active site. Our candidate drugs could fit in more precisely and more accommodating than active site of COX-2. This case can be inferred from binding energies.

These compounds that we identified as COX-2 inhibitors also indicated very reasonable ADMET properties (Figure 4.24).

Detailed analysis of 2D interactions show that nearly all candidates having hydrophobic interactions (π-π or π–cation) with Arg120 and hydrogen bonding with Tyr385 show much better inhibition. All ligands that passed ADMET derived from the same scaffold which has 5 rings in the formula and have very high blood brain barrier penetration which means drug can pass to BBB circulation.

As a concluding remark, the use of computational modeling and screening methods are invaluable tools to search for the right compounds. This procedure provides a method, which saves huge amount of money and shortens time drastically.

We believe that the model compounds that we developed in this study worth trying to synthesize in future work and needs confirmation of experimental studies.

Curriculum Vitae

Tuğba Mehmetoğlu was born in 18 November 1986 in İstanbul. Her B.Sc. degree has been earned in Biology in 2008 from Fatih University. After her undergraduate study, she was accepted to Sabancı University, Biological Sciences and bioengineering graduate program and received M.Sc. in 2010. After a year of working in a drug company, she was accepted to Kadir Has University for a graduate study on Computational Biology and Bioinformatics in February 2011. Computational biology and modeling area is her main interest.

Publications:

1.   Yucebilgili, K., Mehmetoglu, T., Gucin, Z., Salih, B. A..,*Helicobacter pylori DNA in gallbladder tissue of patients with cholelithiasis and cholecystitis.* J Infect Dev Ctries, 2009. **3**(11): p. 856-9.

6. REFERENCES:

1   Kean, W. F. & Buchanan, W. W. The use of NSAIDs in rheumatic disorders 2005: a global perspective. *Inflammopharmacology* **13**, 343-370, doi:10.1163/156856005774415565 (2005).

2   Kore, P. P., Mutha, M. M., Antre, R. V., Oswal, R. J. & Kshirsagar, S. S. Computer-Aided Drug Design: An Innovative Tool for Modeling. (2012).

3   Smith, W. L., DeWitt, D. L. & Garavito, R. M. Cyclooxygenases: structural, cellular, and molecular biology. *Annual review of biochemistry* **69**, 145-182, doi:10.1146/annurev.biochem.69.1.145 (2000).

4   Marcus, A., Gallin, J., Goldstein, I. & Snyderman, R.   (Raven Press, Ltd, New York, 1988).

5   FitzGerald, G. A. COX-2 and beyond: Approaches to prostaglandin inhibition in human disease. *Nature reviews. Drug discovery* **2**, 879-890, doi:10.1038/nrd1225 (2003).

6   McAdam, B. F. *et al.* Effect of regulated expression of human cyclooxygenase isoforms on eicosanoid and isoeicosanoid production in inflammation. *The Journal of clinical investigation* **105**, 1473-1482, doi:10.1172/JCI9523 (2000).

7   Griswold, D. E. & Adams, J. L. Constitutive cyclooxygenase (COX-1) and inducible cyclooxygenase (COX-2): rationale for selective inhibition and progress to date. *Medicinal research reviews* **16**, 181-206, doi:10.1002/(SICI)1098-1128(199603)16:2<181::AID-MED3>3.0.CO;2-X (1996).

8   Iseki, S. Immunocytochemical localization of cyclooxygenase-1 and cyclooxygenase-2 in the rat stomach. *The Histochemical journal* **27**, 323-328 (1995).

9   Wilborn, J., DeWitt, D. L. & Peters-Golden, M. Expression and role of cyclooxygenase isoforms in alveolar and peritoneal macrophages. *The American journal of physiology* **268**, L294-301 (1995).

10   Slater, D. M., Berger, L. C., Newton, R., Moore, G. E. & Bennett, P. R. Expression of cyclooxygenase types 1 and 2 in human fetal membranes at term. *American journal of obstetrics and gynecology* **172**, 77-82 (1995).

11   Komers, R. & Epstein, M. Cyclooxygenase-2 expression and function in renal pathophysiology. *Journal of hypertension. Supplement : official journal of the International Society of Hypertension* **20**, S11-15 (2002).

12   Murakami, M., Matsumoto, R., Austen, K. F. & Arm, J. P. Prostaglandin endoperoxide synthase-1 and -2 couple to different transmembrane stimuli to generate prostaglandin D2 in mouse bone marrow-derived mast cells. *J Biol Chem* **269**, 22269-22275 (1994).

13   Luong, C. *et al.* Flexibility of the NSAID binding site in the structure of human cyclooxygenase-2. *Nature structural biology* **3**, 927-933 (1996).

14   Chandrasekharan, N. V. *et al.* COX-3, a cyclooxygenase-1 variant inhibited by acetaminophen and other analgesic/antipyretic drugs: cloning, structure, and expression. *Proceedings of the National Academy of Sciences of the United States of America* **99**, 13926-13931, doi:10.1073/pnas.162468699 (2002).

15   Picot, D., Loll, P. J. & Garavito, R. M. The X-ray crystal structure of the membrane protein prostaglandin H2 synthase-1. *Nature* **367**, 243-249, doi:10.1038/367243a0 (1994).

16   Duggan, K. C. *et al.* Molecular basis for cyclooxygenase inhibition by the non-steroidal anti-inflammatory drug naproxen. *J Biol Chem* **285**, 34950-34959, doi:10.1074/jbc.M110.162982 (2010).

17   Xie, W., Robertson, D. L. & Simmons, D. L. Mitogen-inducible prostaglandin G/H synthase: A new target for nonsteroidal antiinflammatory drugs. *Drug development research* **25**, 249-265 (1992).

18   Selinsky, B. S., Gupta, K., Sharkey, C. T. & Loll, P. J. Structural analysis of NSAID binding by prostaglandin H2 synthase: time-dependent and time-independent inhibitors elicit identical enzyme conformations. *Biochemistry* **40**, 5172-5180 (2001).

19   Otto, J. C., DeWitt, D. L. & Smith, W. L. N-glycosylation of prostaglandin endoperoxide synthases-1 and -2 and their orientations in the endoplasmic reticulum. *The Journal of biological chemistry* **268**, 18234-18242 (1993).

20   Barnett, J. *et al.* Purification, characterization and selective inhibition of human prostaglandin G/H synthase 1 and 2 expressed in the baculovirus system. *Biochim Biophys Acta* **1209**, 130-139 (1994).

21   DeWitt, D. L. & Meade, E. A. Serum and glucocorticoid regulation of gene transcription and expression of the prostaglandin H synthase-1 and prostaglandin H synthase-2 isozymes. *Arch Biochem Biophys* **306**, 94-102, doi:10.1006/abbi.1993.1485 (1993).

22   Smith, W. L. & Marnett, L. J. Prostaglandin endoperoxide synthase: structure and catalysis. *Biochimica et biophysica acta* **1083**, 1-17 (1991).

23   Shimokawa, T., Kulmacz, R. J., DeWitt, D. L. & Smith, W. L. Tyrosine 385 of prostaglandin endoperoxide synthase is required for cyclooxygenase catalysis. *The Journal of biological chemistry* **265**, 20073-20076 (1990).

24   Marnett, L. J., Rowlinson, S. W., Goodwin, D. C., Kalgutkar, A. S. & Lanzo, C. A. Arachidonic acid oxygenation by COX-1 and COX-2. Mechanisms of catalysis and inhibition. *The Journal of biological chemistry* **274**, 22903-22906 (1999).

25   Landino, L. M., Crews, B. C., Gierse, J. K., Hauser, S. D. & Marnett, L. J. Mutational analysis of the role of the distal histidine and glutamine residues of prostaglandin-endoperoxide synthase-2 in peroxidase catalysis, hydroperoxide reduction, and cyclooxygenase activation. *The Journal of biological chemistry* **272**, 21565-21574 (1997).

26   Seibold, S. A. *et al.* Peroxidase activity in prostaglandin endoperoxide H synthase-1 occurs with a neutral histidine proximal heme ligand. *Biochemistry* **39**, 6616-6624 (2000).

27   Shimokawa, T. & Smith, W. L. Essential histidines of prostaglandin endoperoxide synthase. His-309 is involved in heme binding. *The Journal of biological chemistry* **266**, 6168-6173 (1991).

28   Smith, W. L. & Song, I. The enzymology of prostaglandin endoperoxide H synthases-1 and -2. *Prostaglandins & other lipid mediators* **68-69**, 115-128 (2002).

29   Inoue, T. *et al.* Mechanism of metal activation of human hematopoietic prostaglandin D synthase. *Nature structural biology* **10**, 291-296, doi:10.1038/nsb907 (2003).

30   Kothekar, V., Sahi, S., Srinivasan, M., Mohan, A. & Mishra, J. Recognition of cyclooxygenase-2 (COX-2) active site by NSAIDs: A computer modelling study. *Indian J Biochem Bio* **38**, 56-63 (2001).

31   Euler, A. R. *et al.* Arbaprostil's [15(R)-15-methyl PGE2] effects on intrauterine pressure in the nonpregnant and pregnant human female--a report of four clinical trials. *Prostaglandins, leukotrienes, and essential fatty acids* **38**, 91-98 (1989).

32   Langman, M. J. *et al.* Risks of bleeding peptic ulcer associated with individual non-steroidal anti-inflammatory drugs. *Lancet* **343**, 1075-1078 (1994).

33   Meade, E. A., Smith, W. L. & DeWitt, D. L. Differential inhibition of prostaglandin endoperoxide synthase (cyclooxygenase) isozymes by aspirin and other non-steroidal anti-inflammatory drugs. *J Biol Chem* **268**, 6610-6614 (1993).

34   Warner, T. D. & Mitchell, J. A. Cyclooxygenases: new forms, new inhibitors, and lessons from the clinic. *Faseb J* **18**, 790-804, doi:DOI 10.1096/fj.03-0645rev (2004).

35   Lin, L. L., Lin, A. Y. & DeWitt, D. L. Interleukin-1 alpha induces the accumulation of cytosolic phospholipase A2 and the release of prostaglandin E2 in human fibroblasts. *The Journal of biological chemistry* **267**, 23451-23454 (1992).

36   Marshall, P. J., Kulmacz, R. J. & Lands, W. E. Constraints on prostaglandin biosynthesis in tissues. *The Journal of biological chemistry* **262**, 3510-3517 (1987).

37   Marnett, L. J., Siedlik, P. H. & Fung, L. W. Oxidation of phenidone and BW755C by prostaglandin endoperoxide synthetase. *The Journal of biological chemistry* **257**, 6957-6964 (1982).

38   Hsuanyu, Y. & Dunford, H. B. Prostaglandin H synthase kinetics. The effect of substituted phenols on cyclooxygenase activity and the substituent effect on phenolic peroxidatic activity. *The Journal of biological chemistry* **267**, 17649-17657 (1992).

39   Palomer, A. *et al.* Identification of novel cyclooxygenase-2 selective inhibitors using pharmacophore models. *Journal of medicinal chemistry* **45**, 1402-1411 (2002).

40   Kalgutkar, A. S., Rowlinson, S. W., Crews, B. C. & Marnett, L. J. Amide derivatives of meclofenamic acid as selective cyclooxygenase-2 inhibitors. *Bioorganic & medicinal chemistry letters* **12**, 521-524 (2002).

41   Rainsford, K. D. Anti-inflammatory drugs in the 21st century. *Sub-cellular biochemistry* **42**, 3-27 (2007).

42   Futaki, N. *et al.* NS-398, a new anti-inflammatory agent, selectively inhibits prostaglandin G/H synthase/cyclooxygenase (COX-2) activity in vitro. *Prostaglandins* **47**, 55-59 (1994).

43   Dannhardt, G. & Kiefer, W. Cyclooxygenase inhibitors--current status and future prospects. *European journal of medicinal chemistry* **36**, 109-126 (2001).

44   Docking, D. F. Structure Based Design in Discovery Studio.

45   Böhm, H.-J. The computer program LUDI: a new method for the de novo design of enzyme inhibitors. *Journal of Computer-Aided Molecular Design* **6**, 61-78 (1992).

46   Irwin, J. J. & Shoichet, B. K. ZINC--a free database of commercially available compounds for virtual screening. *J Chem Inf Model* **45**, 177-182, doi:10.1021/ci049714+ (2005).

47   Hou, T., Wang, J., Li, Y. & Wang, W. Assessing the performance of the MM/PBSA and MM/GBSA methods. 1. The accuracy of binding free energy calculations based on molecular dynamics simulations. *Journal of chemical information and modeling* **51**, 69-82 (2010).

48   Eldridge, M. D., Murray, C. W., Auton, T. R., Paolini, G. V. & Mee, R. P. Empirical scoring functions: I. The development of a fast empirical scoring function to estimate the binding affinity of ligands in receptor complexes. *Journal of computer-aided molecular design* **11**, 425-445 (1997).

49   Li, Z. & Scheraga, H. A. Monte Carlo-minimization approach to the multiple-minima problem in protein folding. *Proceedings of the National Academy of Sciences* **84**, 6611-6615 (1987).

50   Rostami-Hodjegan, A. & Tucker, G. T. Simulation and prediction of in vivo drug metabolism in human populations from in vitro data. *Nature reviews. Drug discovery* **6**, 140-148, doi:10.1038/nrd2173 (2007).

51   AKDOĞAN, E. D., Erman, B. & Yelekci, K. In silico design of novel and highly selective lysine-specific histone demethylase inhibitors. *Turk. J. Chem* **35**, 523-542 (2011).

52   Neudert, G. & Klebe, G. DSX: A knowledge-based scoring function for the assessment of protein–ligand complexes. *Journal of chemical information and modeling* **51**, 2731-2745 (2011).

53   Chen, P. Y. *et al.* Computational analysis of novel drugs designed for use as acetylcholinesterase inhibitors and histamine H-3 receptor antagonists for Alzheimer's disease by docking, scoring and de novo evolution. *Mol Med Rep* **5**, 1043-1048, doi:Doi 10.3892/Mmr.2012.757 (2012).

54   Goodsell, D. S., Morris, G. M. & Olson, A. J. Automated docking of flexible ligands: applications of AutoDock. *Journal of Molecular Recognition* **9**, 1-5 (1996).

55   Verdonk, M. L., Cole, J. C., Hartshorn, M. J., Murray, C. W. & Taylor, R. D. Improved protein–ligand docking using GOLD. *Proteins: Structure, Function, and Bioinformatics* **52**, 609-623 (2003).

56   Gupta, K., Selinsky, B. S., Kaub, C. J., Katz, A. K. & Loll, P. J. The 2.0 A resolution crystal structure of prostaglandin H2 synthase-1: structural insights into an unusual peroxidase. *Journal of molecular biology* **335**, 503-518 (2004).

57   O'Boyle, N. M. *et al.* Open Babel: An open chemical toolbox. *J Cheminformatics* **3**, doi:Artn 33 Doi 10.1186/1758-2946-3-33 (2011).

58   Jones, G., Willett, P. & Glen, R. C. Molecular recognition of receptor sites using a genetic algorithm with a description of desolvation. *Journal of molecular biology* **245**, 43-53 (1995).

59   Jones, G., Willett, P., Glen, R. C., Leach, A. R. & Taylor, R. Development and validation of a genetic algorithm for flexible docking. *Journal of molecular biology* **267**, 727-748 (1997).

60   Yelekci, K., Karahan, O. & Toprakci, M. Docking of novel reversible monoamine oxidase-B inhibitors: efficient prediction of ligand binding sites and estimation of inhibitors thermodynamic properties. *Journal of neural transmission* **114**, 725-732, doi:10.1007/s00702-007-0679-7 (2007).

61   Forli, S. AutoDock VS Preparation Tool.

62   Altuntaş, S. *In silico* Design Of Selective Monoamine Oxidase B Inhibitors Using Indane Ring, Kadir Has University, Master Thesis,2013.

63   Hou, T. & Xu, X. Recent development and application of virtual screening in drug discovery: an overview. *Current pharmaceutical design* **10**, 1011-1033 (2004).